

Magneto-optical transport in type-II Weyl semimetals in the presence of orbital magnetic moment

Panchlal Prabhat

Department of Physics, Lalit Narayan Mithila University, Darbhanga, Bihar 846004, India

Amit Gupta

Department of Physics, M. R. M. College, Lalit Narayan Mithila University, Darbhanga, Bihar 846004, India

(Dated: May 12, 2026)

The magneto-optical transport of gapless type-I tilted single Weyl semimetals (WSMs) exhibits suppression of total magnetoconductivities in the presence of orbital magnetic moment (OMM) in linear and nonlinear responses (Yang Gao et al., Phys. Rev. B **105**, 165307 (2022)). In this work, we extend our study to investigate magnetoconductivities in gapless type-II Weyl semimetals within the semiclassical Boltzmann approach and show the differences that arise compared to type-I Weyl semimetals.

I. INTRODUCTION

In 1929, Hermann Weyl hypothesized a novel form of fermion with zero mass and explicit chirality, known as the Weyl fermion (WF) [1]. Weyl semimetals are 3D topological materials that host this WF and have been experimentally realized in condensed matter systems [2–6]. In the Brillouin zone, these materials manifest itself as a pair of conduction and valence bands that touch at a discrete location known as the Weyl points [6–12]. These Weyl points are acting as monopole sources or sinks of Berry curvature, which is typically regarded as an effective magnetic field in momentum space [13, 14].

Constrained by the Nielsen-Ninomiya no-go theorem, the Weyl points (WPs) always appear in pairs of opposing chirality in the momentum space [15]. The Weyl nodes in Weyl semimetals with broken time reversal symmetry arrive in pairs of equal energy, but their chirality is opposite and they are displaced in momentum. Additionally, the Weyl points are no longer at the same energy if inversion symmetry is broken. Several materials like TaAs, NbAs [2, 3], $YbMnBi_2$ [16], $HgCr_2Se_4$ [11] and Pyrochlore iridates [8] have been found to be Weyl semimetals with pairs of Weyl nodes showing opposite chirality. These materials exhibit unique properties namely negative magnetoresistance [5, 17] and surface state with Fermi arcs associated with chiral anomaly [18, 19]. This leads to a variety of intriguing magnetoconductivity (MC) and magneto-thermal transport features in WSM, which have been thoroughly studied theoretically [20–34]. They also exhibit an anomalous Hall effect [10, 23, 35–37].

The Weyl fermions in WSMs are not restricted by Lorentz symmetry, in contrast to their high-energy counterpart, which permits the Weyl cones to tilt in energy-momentum space. When the tilting of the cones is large enough such that the velocity changes sign along the tilting direction, a transition from type-I to type-II WSMs occurs [38–45]. In type-I WSM, the tilt t_s is sup-

posed to be smaller than the Fermi velocity v_F . There is a closed Fermi surface enclosing either electron or a hole pocket, with a single point consistent with Weyl node. However, in type-II WSM, the tilt t_s becomes larger than v_F , the Fermi surface no longer just a point, at the Fermi surface there exists an unbounded electron and hole pockets and even at Weyl point, there are large density of states exist [38], which outcomes in different magnetotransport properties of type-II WSM [20, 21, 36, 46–48].

In this paper, we study the linear and nonlinear magneto-optical responses for tilted type-II WSM in the presence of an orbital magnetic moment (OMM). This has been studied for WSMs without tilt term [49] as well as type-I WSM [50]. The linear response has been studied for type-II WSM without OMM [51]. However, non-linear magnetoconductivity has not been discussed in the literature with the combined effects of both the tilting and orbital magnetic moment terms [52]. The orbital magnetic moment can be thought of as the self-rotation of the Bloch wave packet, and alters the energy of the Bloch electron under the external magnetic field [53]. This orbital moment suppresses the magneto-optical responses of tilted type-I WSM [50]. We derive an analytic expression for the magnetoconductivity employing the semiclassical Boltzmann approach. It is found that the orbital magnetic moment induces a non-trivial magnetoconductivity term, resulting in a partial cancellation of the total magnetoconductivity. This cancellation is more pronounced compared to type-I WSMs. Further, we analyzed this suppressed feature for linear and quadratic contributions in the magnetic field to magnetoconductivities. We also show that the linear-B (quadratic-B) magnetoconductivity exhibits a behavior that is dependent (independent) of the chirality of the Weyl node in both linear or nonlinear response regimes, as in the case of type-I WSMs [50].

The paper is organized as follows: In Sec. II, we begin with the model of a tilted-Weyl semimetal with a tilt in the z direction, and then the semiclassical equations

of motion for the dynamics of the electron wave packet in the electric and magnetic fields are presented. We have reproduced the results and figures of Ref.[50] for type-I WSMs to compare with its type-II WSMs. In Sec. III, the B-linear and quadratic-B magnetoconductivities including the orbital magnetic moment are obtained in the linear response regime, and analyzed in detail. In Sec. IV, we study second harmonic generation, and give the second harmonic conductivity formula as well as the further analysis for this result. We end with conclusions in Sec. V.

II. MODEL HAMILTONIAN AND SEMICLASSICAL BOLTZMANN APPROACH

The non-interacting low-energy effective Hamiltonian for tilted Weyl semimetals is given by [36],

$$\mathcal{H}_0 = \hbar v_F (s \mathbf{k} \cdot \boldsymbol{\sigma} + t_s k_z \sigma_0) \quad (1)$$

where $s = \pm 1$ is the chirality of the Weyl node, \mathbf{k} is the momentum, v_F is the effective velocity, $\boldsymbol{\sigma} \{\sigma_x, \sigma_y, \sigma_z\}$ are the three Pauli matrices and σ_0 is a 2×2 identity matrix, the parameter t_s characterizes the tilting of the Weyl cone. The energy dispersion for tilted WSMs is given by $\epsilon_{\mathbf{k}}^s = \hbar v_F (t_s k_z \pm k)$ with \pm represent for the conduction and valence bands respectively. This Hamiltonian corresponds to type-I WSM only for small tilt parameter $t_s < 1$, such that the Fermi surface encloses only a electron ($\mu > 0$) or a hole ($\mu < 0$) pocket. And for type-II WSM, tilt parameter $t_s > 1$, leading over tilted WNs and at the Fermi energy, the presence of unbounded electron and hole pockets. In type-II WSM, there is finite contribution from both the valence and conduction bands to all physical properties, which is contrast to type-I WSM. We will use semiclassical Boltzmann equations in this study.

In the presence of a static magnetic field \mathbf{B} and a time varying electric field \mathbf{E} , the semiclassical equations of motion at the location \mathbf{r} and the wave-vector \mathbf{k} in a given band are [14, 53]

$$\dot{\mathbf{r}} = \frac{1}{\hbar} \nabla_{\mathbf{k}} \tilde{\epsilon}_{\mathbf{k}}^s - \dot{\mathbf{k}} \times \boldsymbol{\Omega}_{\mathbf{k}}^s \quad (2)$$

$$\hbar \dot{\mathbf{k}} = -e \mathbf{E} - e \dot{\mathbf{r}} \times \mathbf{B} \quad (3)$$

where $-e$ is the electron charge. The first term on the right-hand side of Eq(2) is $\mathbf{v}_{\mathbf{k}}^s = \frac{1}{\hbar} \nabla_{\mathbf{k}} \tilde{\epsilon}_{\mathbf{k}}^s$, defined in terms of an effective band dispersion $\tilde{\epsilon}_s(\mathbf{k})$. In topological metals such as WSMs, this quantity acquires a term due to the intrinsic orbital moment, i.e., $\tilde{\epsilon}_{\mathbf{k}}^s = \epsilon_{\mathbf{k}}^s - \mathbf{m}_{\mathbf{k}}^s \cdot \mathbf{B}$, while $\mathbf{m}_{\mathbf{k}}^s$ is the orbital moment induced by the semiclassical ‘‘self-rotation’’ of the Bloch wavepacket. The terms Berry curvature ($\boldsymbol{\Omega}_{\mathbf{k}}^s$) and orbital magnetic moment ($\mathbf{m}_{\mathbf{k}}^s$) are defined as [14, 53]

$$\boldsymbol{\Omega}_{\mathbf{k}}^s = \text{Im}[\langle \nabla_{\mathbf{k}} u_{\mathbf{k}}^s | \times | \nabla_{\mathbf{k}} u_{\mathbf{k}}^s \rangle] \quad (4)$$

$$\mathbf{m}_{\mathbf{k}}^s = -\frac{e}{2\hbar} \text{Im}[\langle \nabla_{\mathbf{k}} u_{\mathbf{k}}^s | \times (\mathcal{H}_J(\mathbf{k}) - \epsilon_{\mathbf{k}}^s) | \nabla_{\mathbf{k}} u_{\mathbf{k}}^s \rangle] \quad (5)$$

where $|u_{\mathbf{k}}^s\rangle$ satisfies the equation $\mathcal{H}_0(\mathbf{k})|u_{\mathbf{k}}^s\rangle = \epsilon_{\mathbf{k}}^s |u_{\mathbf{k}}^s\rangle$.

The general expressions for Berry curvature and orbital magnetic moment for WSMs are [54]

$$\boldsymbol{\Omega}_{\mathbf{k}}^s = -s \frac{\mathbf{k}}{2k^3} \quad (6)$$

$$\mathbf{m}_{\mathbf{k}}^s = -s e v_F \frac{\mathbf{k}}{2k^2} \quad (7)$$

The two equations (2) and (3) can be decoupled to get

$$\dot{\mathbf{r}} = \frac{1}{\hbar D} [\nabla_{\mathbf{k}} \tilde{\epsilon}_{\mathbf{k}}^s + e \mathbf{E} \times \boldsymbol{\Omega}_{\mathbf{k}}^s] + \frac{e}{\hbar} (\nabla_{\mathbf{k}} \tilde{\epsilon}_{\mathbf{k}}^s \cdot \boldsymbol{\Omega}_{\mathbf{k}}^s) \mathbf{B} \quad (8)$$

$$\hbar \dot{\mathbf{k}} = \frac{1}{\hbar D} [-e \mathbf{E} - \frac{e}{\hbar} \nabla_{\mathbf{k}} \tilde{\epsilon}_{\mathbf{k}}^s \times \mathbf{B} - \frac{e^2}{\hbar} (\mathbf{E} \cdot \mathbf{B}) \boldsymbol{\Omega}_{\mathbf{k}}^s] \quad (9)$$

where the factor $D = 1 + \frac{e}{\hbar} (\boldsymbol{\Omega}_{\mathbf{k}}^s \cdot \mathbf{B})$ modifies the phase space volume [55].

For a given chirality $s = \pm$ of a single Weyl node, the semiclassical Boltzmann equation (SBE) reads as follows

$$\frac{\partial \tilde{f}^s}{\partial t} + \dot{\mathbf{k}} \cdot \frac{\partial \tilde{f}^s}{\partial \mathbf{k}} = \frac{\tilde{f}^s - \tilde{f}_0^s}{\tau} \quad (10)$$

Here, $\tilde{f}^s(\tilde{\epsilon}_{\mathbf{k}}^s)$ is the electron distribution function and τ is the relaxation time originating from the scattering of electrons by phonons, impurities, electrons and other lattice imperfections [56].

The $\tilde{f}_0^s(\epsilon_{\mathbf{k}}^s)$ can be expanded at low magnetic field as [57]

$$\begin{aligned} \tilde{f}_0^s(\tilde{\epsilon}_{\mathbf{k}}^s) &= \tilde{f}_0^s(\epsilon_{\mathbf{k}}^s - \mathbf{m}_{\mathbf{k}}^s \cdot \mathbf{B}) \\ &\simeq \tilde{f}_0^s(\epsilon_{\mathbf{k}}^s) - \mathbf{m}_{\mathbf{k}}^s \cdot \mathbf{B} \frac{\partial \tilde{f}_0^s(\epsilon_{\mathbf{k}}^s)}{\partial \epsilon_{\mathbf{k}}^s} \end{aligned} \quad (11)$$

where $\tilde{f}_0^s(\epsilon_{\mathbf{k}}^s) = 1/[e^{(\epsilon_{\mathbf{k}}^s - \mu)/k_B T} + 1]$ with k_B the Boltzmann constant, T the temperature, and μ the chemical potential.

Eq.(10) can be solved by expanding the distribution function as a power series in the electric field as

$$\tilde{f}^s = \tilde{f}_0^s + \tilde{f}_1^s e^{-i\omega t} + \tilde{f}_2^s e^{-2i\omega t} + \dots \quad (12)$$

where \tilde{f}_1^s and \tilde{f}_2^s are the first- and second-order terms for \mathbf{E} , respectively. The electric current density can be calculated by

Solved for \tilde{f}_1^s , we obtain

$$\mathbf{j} = -\frac{e}{(2\pi)^3} \int d^3k D \hat{\mathbf{r}} \tilde{f}^s \quad (13)$$

Equation(13) compute the conductivity components under the combined influence of external electric and magnetic fields.

III. LINEAR RESPONSE OF TILTED WSMS

For linear electric field response, we retain only the first two terms of Eq.(12) and substitute Eq.(8) in Eq.(10)

$$\frac{1}{\hbar D} \left[-e\mathbf{E} - \frac{e^2}{\hbar} (\mathbf{E} \cdot \mathbf{B}) \Omega_{\mathbf{k}}^s \right] \cdot \frac{\partial \tilde{f}_0^s}{\partial \mathbf{k}} - i\omega \tilde{f}_1^s = -\frac{\tilde{f}_1^s}{\tau} \quad (14)$$

We expand Eq.(15) up to the second order in magnetic field and obtain

$$\begin{aligned} \tilde{f}_1^s = & \frac{\tau}{(1-i\omega\tau)} \left[e\mathbf{E} \cdot \mathbf{v}_{\mathbf{k}}^s \cdot \frac{\partial \tilde{f}_0^s}{\partial \epsilon_{\mathbf{k}}^s} - \frac{e^2}{\hbar} (\mathbf{B} \cdot \Omega_{\mathbf{k}}^s) (\mathbf{E} \cdot \mathbf{v}_{\mathbf{k}}^s) \frac{\partial \tilde{f}_0^s}{\partial \epsilon_{\mathbf{k}}^s} + \frac{e^2}{\hbar} (\mathbf{E} \cdot \mathbf{B}) (\Omega_{\mathbf{k}}^s \cdot \mathbf{v}_{\mathbf{k}}^s) \frac{\partial \tilde{f}_0^s}{\partial \epsilon_{\mathbf{k}}^s} - \frac{e}{\hbar} \mathbf{E} \cdot \frac{\partial}{\partial \mathbf{k}} \left(\mathbf{m}_{\mathbf{k}}^s \cdot \mathbf{B} \frac{\partial \tilde{f}_0^s}{\partial \epsilon_{\mathbf{k}}^s} \right) \right. \\ & - \frac{e^3}{\hbar^2} (\mathbf{B} \cdot \Omega_{\mathbf{k}}^s) (\mathbf{E} \cdot \mathbf{B}) (\Omega_{\mathbf{k}}^s \cdot \mathbf{v}_{\mathbf{k}}^s) \frac{\partial \tilde{f}_0^s}{\partial \epsilon_{\mathbf{k}}^s} + \frac{e^3}{\hbar^2} (\mathbf{B} \cdot \Omega_{\mathbf{k}}^s)^2 (\mathbf{E} \cdot \mathbf{v}_{\mathbf{k}}^s) \frac{\partial \tilde{f}_0^s}{\partial \epsilon_{\mathbf{k}}^s} + \frac{e^2}{\hbar^2} (\mathbf{B} \cdot \Omega_{\mathbf{k}}^s) \mathbf{E} \cdot \frac{\partial}{\partial \mathbf{k}} \left(\mathbf{m}_{\mathbf{k}}^s \cdot \mathbf{B} \frac{\partial \tilde{f}_0^s}{\partial \epsilon_{\mathbf{k}}^s} \right) \\ & \left. - \frac{e^2}{\hbar^2} \Omega_{\mathbf{k}}^s \cdot \frac{\partial}{\partial \mathbf{k}} \left(\mathbf{m}_{\mathbf{k}}^s \cdot \mathbf{B} \frac{\partial \tilde{f}_0^s}{\partial \epsilon_{\mathbf{k}}^s} \right) \right] \end{aligned} \quad (16)$$

From Eqs.(8) and Eq.(16), the expression for current density at time t is given by

$$\begin{aligned} \mathbf{j}_1 = & -\frac{e}{(2\pi)^3} \int d^3k \left[\tilde{\mathbf{v}}_{\mathbf{k}}^s + \frac{e}{\hbar} (\Omega_{\mathbf{k}}^s \cdot \tilde{\mathbf{v}}_{\mathbf{k}}^s) \mathbf{B} \right] \tilde{f}_1^s \\ & - \frac{e^2}{2\pi^3 \hbar} \int d^3k \mathbf{E} \times \Omega_{\mathbf{k}}^s \tilde{f}_0^s \end{aligned} \quad (17)$$

The above equation can be expressed in frequency space ω as

$$j_a(\omega) = \sigma_{ab}(\omega) E_b(\omega) \quad (18)$$

where $\sigma_{ab}(\omega)$ is the frequency dependent conductivity. It is known that the single contribution from the group velocity $\tilde{\mathbf{v}}_{\mathbf{k}}^s$ or the Berry curvature $\Omega_{\mathbf{k}}^s$ form the conventional longitudinal or Hall conductivities. In the presence of the magnetic field, the conductivity $\sigma(\omega)$ consists of

the coupling terms between the group velocity $\tilde{\mathbf{v}}_{\mathbf{k}}^s$ and the Berry curvature $\Omega_{\mathbf{k}}^s$ besides the conventional ingredients [see Eq. (17)]. Their combined contributions are triggered by the external magnetic field and play a crucial role in the electron transport.

A. Calculations of longitudinal conductivities components without magnetic field

Substituting Eq.(16) without \mathbf{B} terms into the first term of Eq.(17), we get longitudinal conductivities components

$$\sigma_{ab}^{(0)}(\omega) = \frac{\tau}{(1-i\omega\tau)} \frac{e^2}{(2\pi)^3} \int d^3k v_a^s v_b^s \left(-\frac{\partial \tilde{f}_0^s}{\partial \epsilon_{\mathbf{k}}^s} \right) \quad (19)$$

$$\sigma_{zz}^0(\omega) = \frac{3\sigma_D}{2t_s^3} \left[-2t_s - \ln \frac{1-t_s}{1+t_s} \right] \quad (20)$$

$$\sigma_{xx}^0(\omega) = \sigma_{yy}^0(\omega) = \frac{3\sigma_D}{4t_s^3} \left[\frac{2t_s}{(1-t_s^2)} + \ln \frac{1-t_s}{1+t_s} \right] \quad (21)$$

At T=0 K, $-\frac{\partial \tilde{f}_0^s}{\partial \epsilon_{\mathbf{k}}^s} = \delta(\epsilon_{\mathbf{k}}^s - \mu)$, we get
For type-I,

For type-II,

$$\sigma_{zz}^0(\omega) = \frac{3\sigma_D}{2|t_s|^5} \left[3 - t_s^2 + (t_s^2 - 1)^2 \tilde{\Lambda}_k^2 + \ln[(t_s^2 - 1) \tilde{\Lambda}_k^2] \right] \quad (22)$$

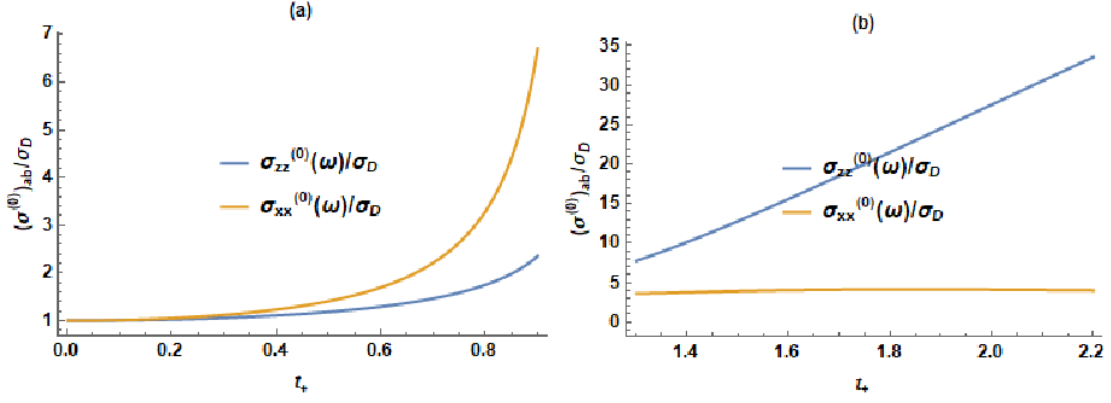


FIG. 1. The dependence of the optical conductivity on the tilt t_+ at zero B field for (a) type-I WSM and (b) type-II WSM. The other parameters are taken as $\tilde{\Lambda}_k = 4, v_F = 4.13 \times 10^5$ m / s, $\mu = 1$ meV and $\tau = 10^{-13}$ s.

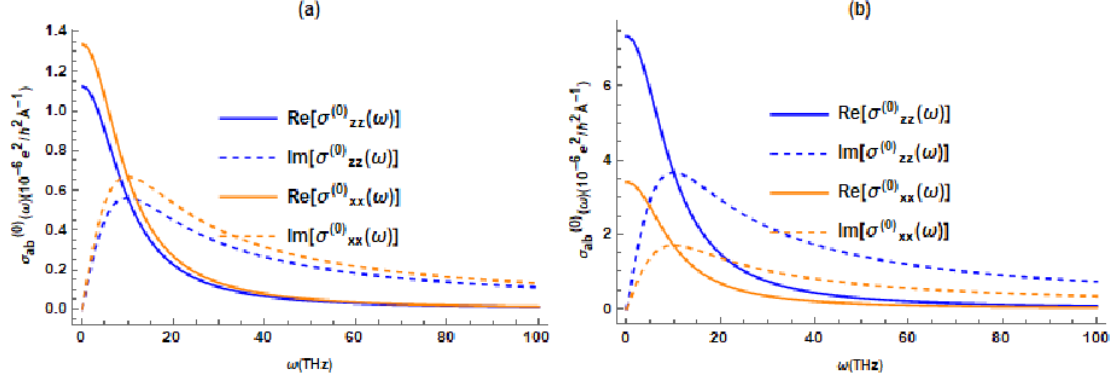


FIG. 2. The frequency dependence of optical conductivity at zero B-field for (a) type-I WSM at $t_s = 0.5$ and (b) type-II WSM at $t_s = 1.3$. The other parameters are the same as those of Fig.(1).

$$\sigma_{xx}^0(\omega) = \frac{3\sigma_D}{4|t_s|^5} \left[\frac{3-t_s^2}{t_s^2-1} + (t_s^2-1)\tilde{\Lambda}_k^2 - \ln[(t_s^2-1)] - 2\ln\tilde{\Lambda}_k \right] \text{conductivity components are shown in Fig.(2).} \quad (23)$$

where $\sigma_D = \frac{e^2\tau\mu^2}{(1-i\omega\tau)6\pi^2\hbar^3v_F}$ is Drude frequency complex conductivity and $\Lambda_k/k_F \equiv \tilde{\Lambda}_k$ is the momentum cut-off to solve conductivity elements in spherical polar coordinates (see Appendix A). Our results of conductivity elements for type-II WSMs are written irrespective of the sign of the tilt parameter t_s . This helps us to understand even and odd nature conductivity elements of the system. Unlike the case of type-I WSM, for a type-II WSM we find that $\sigma_{zz}(0)$ is larger and more sensitive to t_s as compared to $\sigma_{xx}(0)$ [Fig.1] [51]. The frequency dependence of

B. Calculations of conductivity components linear in magnetic field

Substituting Eq.(16) with \mathbf{B} terms up to first order into the first term of Eq.(17), we get conductivity components

$$\sigma_{ab}^{(B)}(\omega) = \sigma_{ab}^{(B,\Omega)}(\omega) + \sigma_{ab}^{(B,m)}(\omega) \quad (24)$$

where

$$\sigma_{ab}^{(B,\Omega)}(\omega) = \frac{\tau}{\hbar(1-i\omega\tau)} \frac{e^3}{(2\pi)^3} \int d^3k [(v_a^s B_b + v_b^s B_a)(\Omega_{\mathbf{k}}^s \cdot \mathbf{v}_{\mathbf{k}}^s) - v_a^s v_b^s (\Omega_{\mathbf{k}}^s \cdot \mathbf{B})] \left(-\frac{\partial f_0^s}{\partial \epsilon_{\mathbf{k}}^s} \right) \quad (25)$$

$$\sigma_{ab}^{(B,m)}(\omega) = \frac{\tau}{\hbar(1-i\omega\tau)} \frac{e^2}{(2\pi)^3} \int d^3k \left[\frac{\partial v_a^s}{\partial k_b} (\mathbf{m}_{\mathbf{k}}^s \cdot \mathbf{B}) - \frac{\partial (\mathbf{m}_{\mathbf{k}}^s \cdot \mathbf{B})}{\partial k_a} v_b^s \right] \left(-\frac{\partial f_0^s}{\partial \epsilon_{\mathbf{k}}^s} \right) \quad (26)$$

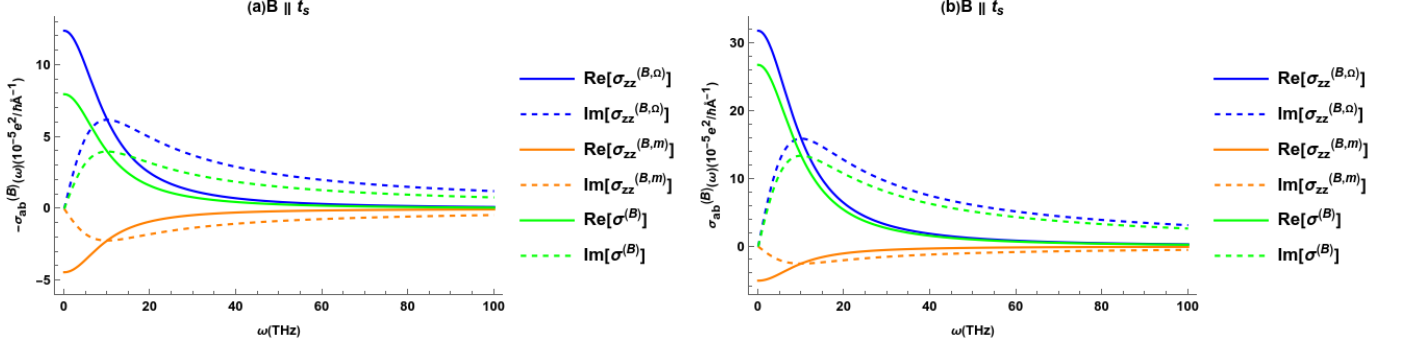


FIG. 4. The dependence of the optical conductivity at $B=1$ on the tilt t_+ for (a) type-I WSM at $t_s = 0.5$ and (b) type-II WSM at $t_s = 1.3$. The other parameters are the same as those of Fig.(1)

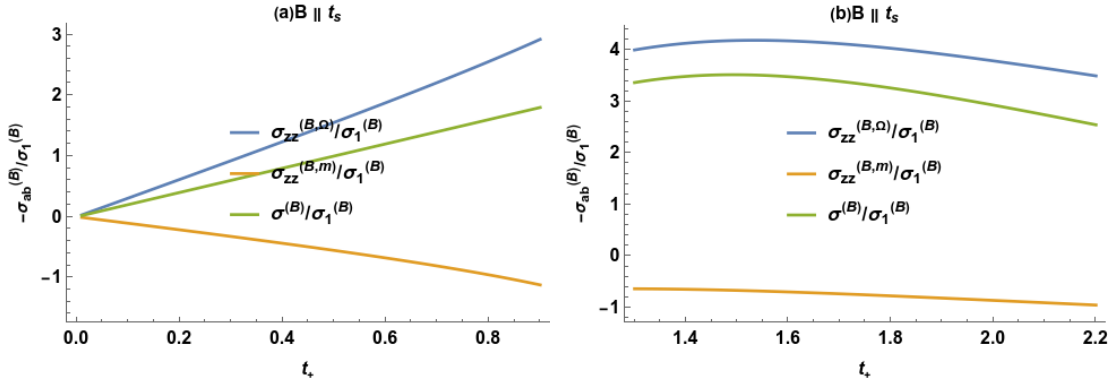


FIG. 3. The dependence of the optical conductivity at $B=1$ on the tilt t_+ for (a) type-I WSM and (b) type-II WSM. The other parameters are the same as those of Fig.(1)

We can easily check from Eqs.(25) and (26) that $\sigma_{ab}^{(B)}(\omega) = \sigma_{ba}^{(B)}(\omega)$. The system possesses the time-reversal symmetry without tilt term and therefore conductivities will vanish [49, 50]. However, the time-reversal symmetry is broken for a finite value of tilt $t_s \neq 0$. The first term and the second term in Eq.(24) is related to the Berry curvature $\Omega_{\mathbf{k}}^s$ and the orbital

magnetic moment $m_{\mathbf{k}}^s$ respectively and has been studied in details for type-I WSMs [50]. In the following, the detailed analysis of Eqs. (25) and (26) are given by considering the magnetic field \mathbf{B} perpendicular and parallel to the tilt direction t_s .

Case-I When $\mathbf{B} \parallel \hat{t}_s \parallel \hat{z}$

In this case, Hall conductivities components are zero and one can get the following expressions for longitudinal components.

For Type-I

$$\sigma_{zz}^{(B,\Omega)} = \sigma_1^{(B)} s \left[\frac{2(3 - 5t_s^2 - 3t_s^4)}{3t_s^3} + \frac{(t_s^2 - 1)^2}{t_s^4} \ln \frac{1 - t_s}{1 + t_s} \right] \quad (27)$$

$$\sigma_{xx}^{(B,\Omega)} = \sigma_1^{(B)} s \left[\frac{2t_s^2 - 3}{3t_s^3} - \frac{1 - t_s^2}{2t_s^4} \ln \frac{1 - t_s}{1 + t_s} \right] \quad (28)$$

for Type-II

$$\begin{aligned} \sigma_{zz}^{(B,\Omega)} &= \frac{\sigma_1^{(B)} s}{3t_s^4} \left[-4\tilde{\Lambda}_k^{-3} + 3(-3 + 2t_s^2)\tilde{\Lambda}_k^{-2} + 36(-1 + t_s^2)\Lambda_k^{-1} + \left\{ -11 + |t_s| \{12 + t_s(21 - 4|t_s|(5 + 3|t_s|))\} \right\} \right. \\ &\quad \left. + 3(t_s^2 - 1)^2 \left\{ 3 \ln(-1 + |t_s|) - \ln(1 + |t_s|) + 2 \ln \tilde{\Lambda}_k \right\} \right] \end{aligned} \quad (29)$$

$$\sigma_{xx}^{(B,\Omega)} = \frac{\sigma_1^{(B)} s}{6t_s^4} \left[-9\tilde{\Lambda}_k^{-2} + (-11 + 9t_s^2) - 3(-1 + t_s^2) \ln[(t_s^2 - 1)\tilde{\Lambda}_k^2] \right] \quad (30)$$

Via the similar calculation, Eq.(26) becomes for Type-I

$$\sigma_{zz}^{(B,m)}(\omega) = \sigma_1^{(B)} s \left[\frac{2(-3 + 5t_s^2)}{3t_s^3} - \frac{(t_s^2 - 1)^2}{t_s^4} \ln \frac{1 - t_s}{1 + t_s} \right] \quad (31)$$

$$\sigma_{xx}^{(B,m)}(\omega) = \sigma_1^{(B)} s \left[\frac{(3 - 8t_s^2)}{3t_s^3} + \frac{1 - 3t_s^2}{2t_s^4} \ln \frac{1 - t_s}{1 + t_s} \right] \quad (32)$$

for Type-II

$$\sigma_{zz}^{(B,m)}(\omega) = \frac{\sigma_1^{(B)} s}{6t_s^4} \left[\tilde{\Lambda}_k^{-2}(-9 + 6t_s^2) + (-11 + 21t_s^2 - 6t_s^4) + 3(-1 + t_s^2)^2 \ln[(t_s^2 - 1) \ln \tilde{\Lambda}_k^2] \right] \quad (33)$$

$$\sigma_{xx}^{(B,m)}(\omega) = \frac{\sigma_1^{(B)} s}{6t_s^4} \left[-2\tilde{\Lambda}_k^{-3} + 18(-1 + t_s^2)\tilde{\Lambda}_k^{-1} + 2|t_s|(3 - 8t_s^2) - 3(-1 + 3t_s^2) \ln \frac{|t_s| - 1}{|t_s| + 1} \right] \quad (34)$$

where $\sigma_1^{(B)} = \frac{e^3 \tau B v_F}{(1 - i\omega\tau) 8\pi^2 \hbar^2}$. From Eqs.(27)-(34) unlike the case of type-I WSM, there is Fermi energy dependence that is tied to the cutoff. The total linear-B contribution of two nodes having parallel tilt becomes zero. But for nodes having opposite tilt as is usually

the case, the total contribution is nonzero. The total conductivities are suppressed(enhanced) in type-I(II) Weyl semimetals. Their tilt and frequency dependence are shown in Fig.(3) to (6).

Case-II For $\mathbf{B} \perp \hat{t}_s(\parallel \hat{z})$

We can represent the magnetic field in the x-y plane as $\mathbf{B} = B(\cos \gamma \hat{i} + \sin \gamma \hat{j})$, where γ is the angle between magnetic field \mathbf{B} and x-axis. In this case, longitudinal components of conductivities are zero and we get the

following expressions for planar Hall conductivities [50, 51]

$$\sigma_{xz}^{(B)}(\omega) = [\sigma^{(B,\Omega)}(\omega) + \sigma^{(B,m)}(\omega)] \cos \gamma \quad (35)$$

$$\sigma_{yz}^{(B)}(\omega) = [\sigma^{(B,\Omega)}(\omega) + \sigma^{(B,m)}(\omega)] \sin \gamma \quad (36)$$

$$\sigma_{xz}^{(B,\Omega)}(\omega) = \frac{\tau}{\hbar(1 - i\omega\tau)} \frac{e^3}{(2\pi)^3} \int d^3k [v_z^s B \cos \gamma (v_y^s \Omega_{ky} + v_z^s \Omega_{kz}) - v_z^s B \sin \gamma v_x^s \Omega_{ky}] \left(-\frac{\partial f_0^s}{\partial \epsilon_{\mathbf{k}}^s} \right) \quad (37)$$

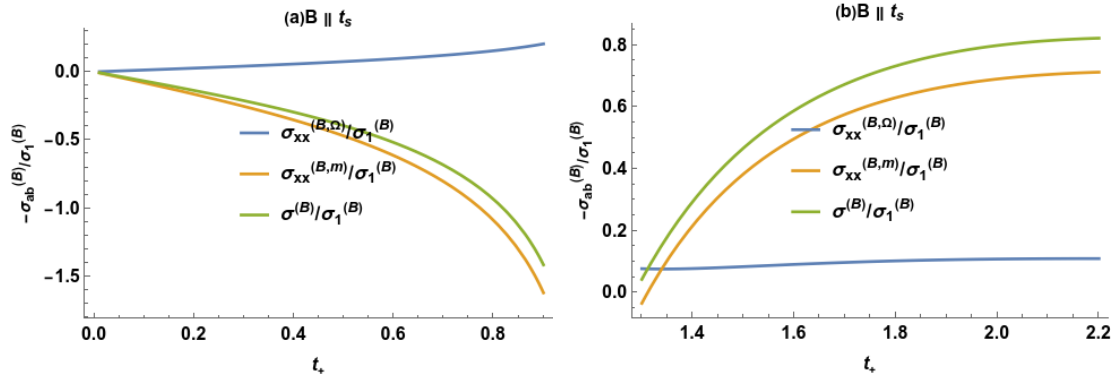


FIG. 5. The dependence of the optical conductivity at $B=1$ on the tilt t_+ for (a) type-I WSM and (b) type-II WSM. The other parameters are the same as those of Fig.(1)

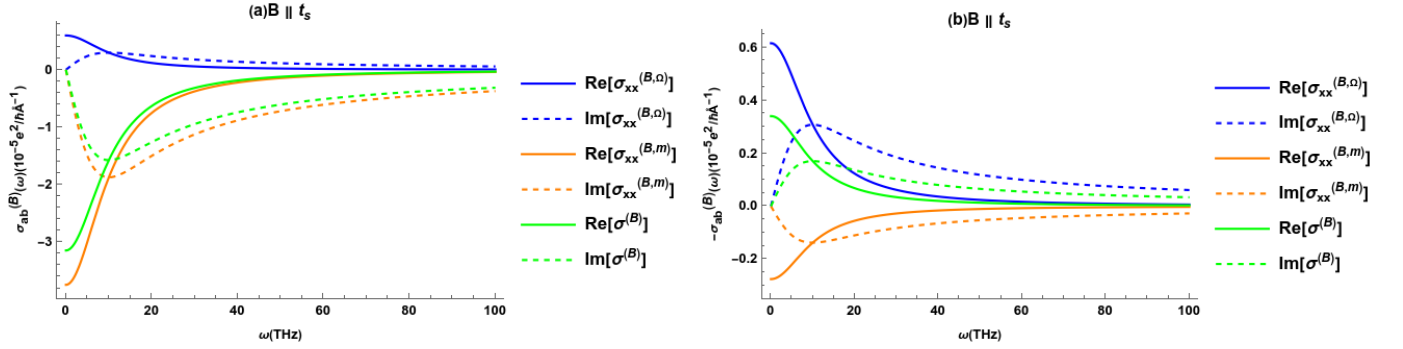


FIG. 6. The dependence of the optical conductivity at $B=1$ on the tilt t_+ for (a) type-I WSM at $t_s = 0.5$ and (b) type-II WSM at $t_s = 1.3$. The other parameters are the same as those of Fig.(1)

$$\sigma_{xz}^{(B,m)}(\omega) = \frac{\tau}{\hbar(1-i\omega\tau)} \frac{e^2}{(2\pi)^3} \int d^3k \left[B \cos \gamma \left(\frac{\partial v_x^s}{\partial k_z} m_{kx}^s - v_z^s \frac{\partial m_{kx}^s}{\partial k_z} \right) - B \sin \gamma \left(\frac{\partial v_x^s}{\partial k_z} m_{ky}^s - v_z^s \frac{\partial m_{ky}^s}{\partial k_x} \right) \right] \left(-\frac{\partial f_0^s}{\partial \epsilon_k^s} \right) \quad (38)$$

The second term of both the above equations contributes to zero.

for Type-I

$$\sigma^{(B,\Omega)} = \sigma_1^{(B)} s \left[\frac{-3 + 5t_s^2 - 6t_s^4}{3t_s^3} - \frac{(1-t_s^2)^2}{2t_s^4} \ln \frac{1-t_s}{1+t_s} \right] \quad (39)$$

$$\sigma^{(B,m)} = \sigma_1^{(B)} s \left[-\frac{2t_s^2 - 3}{3t_s^3} + \frac{1-t_s^2}{2t_s^4} \ln \frac{1-t_s}{1+t_s} \right] \quad (40)$$

for Type-II

$$\sigma^{(B,\Omega)} = \frac{\sigma_1^{(B)} s}{6t_s^4} \left[-2\tilde{\Lambda}_k^{-3} + 6(-3 + 2t_s^2)\tilde{\Lambda}_k^{-2} + 18(-1 + t_s^2)\tilde{\Lambda}_k^{-1} - 2(1 + |t_s|) \{ 11 + |t_s|(-14 + |t_s|(-7 + 12|t_s|)) \} \right. \\ \left. + 3(-1 + t_s^2)^2 \{ 3 \ln(-1 + t_s) + \ln(1 + t_s) - 4 \ln \tilde{\Lambda}_k \} \right] \quad (41)$$

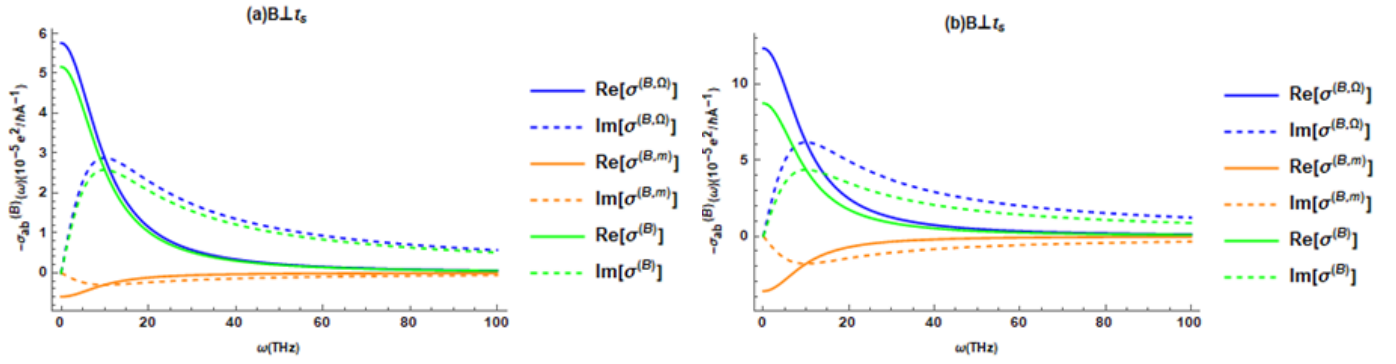


FIG. 8. The frequency dependence of optical conductivity at $B = 1$ T for (a) type-I WSM at $t_s = 0.5$ and (b) type-II WSM at $t_s = 1.3$. The other parameters are the same as those of Fig(1).

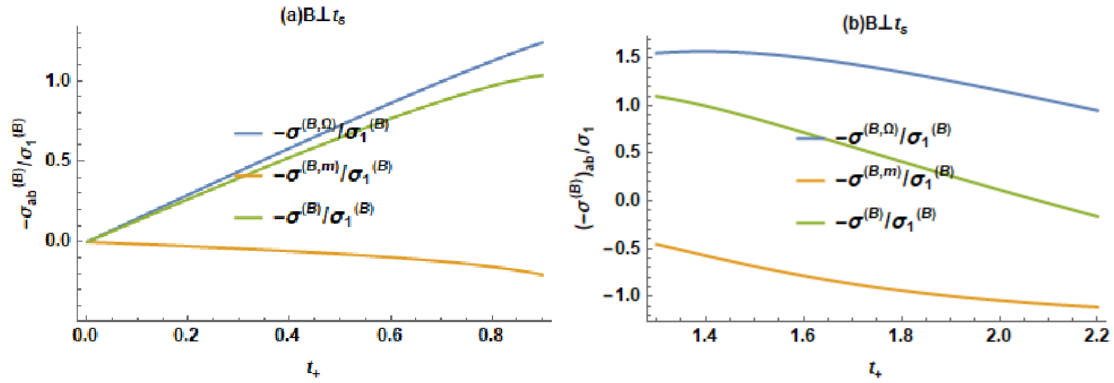


FIG. 7. The dependence of the optical conductivity at $B=1$ on the tilt t_+ for (a) type-I WSM and (b) type-II WSM. The other parameters are the same as those of Fig(1).

$$\begin{aligned} \sigma^{(B, m)} = & \frac{\sigma_1^{(B)} s}{6t_s^4} \left[2 \left\{ \tilde{\Lambda}_k^{-3} - 3(-3 + t_s^2) \tilde{\Lambda}_k^{-2} - 3(-3 + t_s^2) \tilde{\Lambda}_k^{-1} + \{ 11 + |t_s|(-3 + t_s(-12 + |t_s|(2 + 3|t_s|))) \} \right\} \right. \\ & \left. + 3(-1 + t_s^2) \left\{ 3 \ln(-1 + |t_s|) + \ln(1 + |t_s|) - 4 \ln \tilde{\Lambda}_k \right\} \right] \end{aligned} \quad (42)$$

The linear dependence of the rest of the conductivities is zero, i.e., $\sigma_{xy} = \sigma_{xx} = \sigma_{yy} = \sigma_{zz} = 0$.

From Eqs.(27) to (42), we notice that the B-linear magnetoconductivity in type-I/II-Weyl semimetals is independent/dependent of Fermi energy that tied to the cut off and the odd function of t_s [50]. According to the Nielsen-Ninomiya theorem [58], the Weyl nodes with opposite chirality always appears in pairs. The total

magnetoconductivity of the system is the sum of all the Weyl nodes. Therefore, for the case of $t_+ = t_-$, where the tilt inversion symmetry is broken, the contribution of the Weyl node to the magnetoconductivity has the opposite sign for the opposite (B) chirality, giving rise to $\sigma_{ab}(\omega) = 0$. Whereas, for the case of $t_+ = -t_-$, where the tilt inversion symmetry is unbroken, each Weyl node produces an identical contribution to the magnetoconductivity, and so the nonzero magnetocon-

ductivity emerges for this case. Fig.(7) and (8) show the tilt and frequency variations of linear B longitudinal conductivity components for type-I and type-II WSMs respectively. In case of type-II WSMs, the conductivity contribution due to Berry curvature and OMM are more pronounced compared to its type-I one and suppression takes place. Key type-II Weyl materials used for studying PHE include WTe_2 and $MoTe_2$, which serve as ideal platforms for experimental verification. These materials showed pronounced signature of nontrivial Berry-curvature-induced PHE [64, 65]. The planar Hall effect amplitude in WTe_2 is linearly dependent on the magnetic fields [65].

C. Calculations of quadratic-B contribution to the conductivity $\sigma_{ab}^{(B^2)}$

Substituting Eq.(16) with \mathbf{B} terms up to second order into the first term of Eq.(17), we get conductivities components

$$\sigma_{ab}^{(B^2)}(\omega) = \sigma_{ab}^{(B^2,\Omega)}(\omega) + \sigma_{ab}^{(B^2,m)}(\omega) \quad (43)$$

where

$$\begin{aligned} \sigma_{ab}^{(B^2,\Omega)}(\omega) = & \frac{\tau}{\hbar^2(1-i\omega\tau)} \frac{e^4}{(2\pi)^3} \int d^3k [v_a^s v_b^s (\Omega_{\mathbf{k}}^s \cdot \mathbf{B})^2 - (v_a^s B_b + v_b^s B_a) (\Omega_{\mathbf{k}}^s \cdot \mathbf{v}_{\mathbf{k}}^s) (\Omega_{\mathbf{k}}^s \cdot \mathbf{B}) \\ & + B_a B_b (\Omega_{\mathbf{k}}^s \cdot \mathbf{v}_{\mathbf{k}}^s)^2] \left(-\frac{\partial f_0^s}{\partial \epsilon_{\mathbf{k}}^s} \right) \end{aligned} \quad (44)$$

$$\begin{aligned} \sigma_{ab}^{(B^2,m)}(\omega) = & \frac{\tau}{\hbar^2(1-i\omega\tau)} \frac{e^3}{(2\pi)^3} \int d^3k \left[\frac{\partial}{\partial \mathbf{k}} \cdot [v_a^s B_b \Omega_{\mathbf{k}}^s] (\mathbf{m}_{\mathbf{k}}^s \cdot \mathbf{B}) - \frac{\partial [v_a^s (\Omega_{\mathbf{k}}^s \cdot \mathbf{B})]}{\partial k_b} (\mathbf{m}_{\mathbf{k}}^s \cdot \mathbf{B}) + \frac{\partial [B_a (\Omega_{\mathbf{k}}^s \cdot \mathbf{v}_{\mathbf{k}}^s)]}{\partial k_b} (\mathbf{m}_{\mathbf{k}}^s \cdot \mathbf{B}) + \right. \\ & \left. \frac{\partial (\mathbf{m}_{\mathbf{k}}^s \cdot \mathbf{B})}{\partial k_a} (\Omega_{\mathbf{k}}^s \cdot \mathbf{B}) v_b^s - \frac{\partial (\mathbf{m}_{\mathbf{k}}^s \cdot \mathbf{B})}{\partial k_a} (\Omega_{\mathbf{k}}^s \cdot \mathbf{v}_{\mathbf{k}}^s) B_b^s - \frac{\partial^2 (\mathbf{m}_{\mathbf{k}}^s \cdot \mathbf{B})}{e \partial k_a \partial k_b} (\mathbf{m}_{\mathbf{k}}^s \cdot \mathbf{B}) - B_a \frac{\partial (\mathbf{m}_{\mathbf{k}}^s \cdot \mathbf{B})}{\partial \mathbf{k}} \cdot \Omega_{\mathbf{k}}^s v_b^s \right] \left(-\frac{\partial f_0^s}{\partial \epsilon_{\mathbf{k}}^s} \right) \end{aligned} \quad (45)$$

where $\sigma_{ab}^{(B^2,\Omega)}(\omega)$ and $\sigma_{ab}^{(B^2,m)}(\omega)$ are Berry-curvature $\Omega_{\mathbf{k}}^s$ and the orbital magnetic moment $\mathbf{m}_{\mathbf{k}}^s$ dependent conductivities respectively. Consider the following two cases.

Case-I When $\mathbf{B} \parallel \hat{\mathbf{t}}_s \parallel \hat{\mathbf{z}}$

In this case, Hall conductivities components are zero and one can get the following expressions for longitudinal components.

for Type-I

$$\sigma_{zz}^{(B^2,\Omega)}(\omega) = 8\sigma_1^{(B^2)} \quad (46)$$

$$\sigma_{xx}^{(B^2,\Omega)}(\omega) = \sigma_1^{(B^2)} \quad (47)$$

for Type-II

$$\begin{aligned} \sigma_{zz}^{(B^2,\Omega)}(\omega) = & \frac{\sigma_1^{(B^2)}}{2|t_s|^5} \left[-5\tilde{\Lambda}_k^{-6} + 15(-3+t_s^2)\tilde{\Lambda}_k^{-4} \right. \\ & \left. - 15(-1+t_s^2)^2\tilde{\Lambda}_k^{-2} + \left\{ 1 + 5t_s^2(-1+3t_s^2+t_s^4) \right\} \right] \end{aligned} \quad (48) \text{ for Type-II}$$

$$\begin{aligned} \sigma_{xx}^{(B^2,\Omega)}(\omega) = & \frac{\sigma_1^{(B^2)}}{8|t_s|^5} \left[10\tilde{\Lambda}_k^{-6} - 15(-6+t_s^2)\tilde{\Lambda}_k^{-4} \right. \\ & \left. - 30(-1+t_s^2)\tilde{\Lambda}_k^{-2} + (-2+5(t_s^2+t_s^6)) \right] \end{aligned} \quad (49)$$

Considering the effect of the orbital magnetic moment, we have

for Type-I

$$\sigma_{zz}^{(B^2,m)}(\omega) = (-3+5t_s^2)\sigma_1^{(B^2)} \quad (50)$$

$$\sigma_{xx}^{(B^2,m)}(\omega) = -\sigma_1^{(B^2)} \quad (51)$$

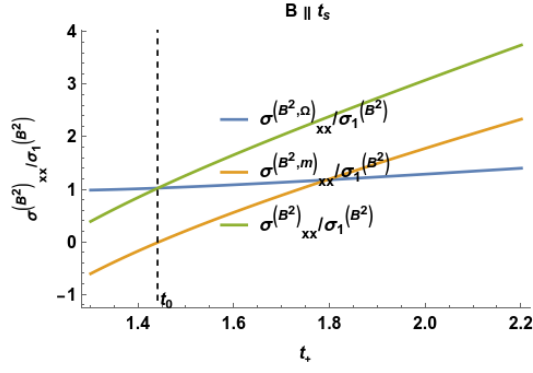


FIG. 9. The dependence of the optical conductivity on the tilt t_+ for the case of $\mathbf{B} \parallel t_s$ for type-II WSM. The other parameters are the same as those of Fig.(1).

$$\begin{aligned} \sigma_{zz}^{(B^2, m)}(\omega) &= \frac{\sigma_1^{(B^2)}}{16|t_s|^5} \left[320\tilde{\Lambda}_k^{-6} + 384\tilde{\Lambda}_k^{-5} + 60(48 - 7t_s)\tilde{\Lambda}_k^{-4} - 160(-4 + t_s^2)\tilde{\Lambda}_k^{-3} + 15(64 - 56t_s^2 - 3t_s^4)\tilde{\Lambda}_k^{-2} \right. \\ &\quad \left. + \left\{ -64 + 140t_s^2 + t_s^4 \{ 35 + |t_s|(-374 + 295|t_s|) \} \right\} \right] \end{aligned} \quad (52)$$

$$\sigma_{xx}^{(B^2, m)}(\omega) = \frac{-\sigma_1^{(B^2)}}{2|t_s|^5} \left[20\tilde{\Lambda}_k^{-6} + 24\tilde{\Lambda}_k^{-5} - 15(-12 + t_s^2)\tilde{\Lambda}_k^{-4} + 40\tilde{\Lambda}_k^{-3} - 30(-2 + t_s^2)\tilde{\Lambda}_k^{-2} + (-4 + 5t_s^2 + 6t_s^5 - 5t_s^6) \right] \quad (53)$$

where $\sigma_1^{(B^2)} = \frac{e^4 \tau B^2 v_F^3}{8\pi^2 \hbar (1 - i\omega\tau) 15\mu^2}$. Obviously, from Eqs.(46) and (53), $\sigma_{xx}^{(B^2, \Omega)}(\omega)$ and $\sigma_{xx}^{(B^2, m)}(\omega)$ are equal and opposite values, thus the total conductivity $\sigma_{xx}^{(B^2)}(\omega)$ is equal to zero in the case of type-I WSM [50]. However, there is no such cancellation happens for type-II case and total conductivity is enhanced above the value of $t_0 (= 1.44)$ due to OMM as shown in Fig.(9). Fur-

thermore, in the case of type-I WSM, the total conductivity component $\sigma_{zz}^{(B^2)}(\omega)$ is suppressed(enhanced) below(above) the value of t_0 as shown in Fig.(10a)(see ref.[50]). For type-II WSM, the conductivity component $\sigma_{zz}^{(B^2)}(\omega)$ is enhanced with tilt parameter t_+ as shown in Fig.(10b) due to positive contribution of OMM component.

Case-II For $\mathbf{B} \perp \hat{t}_s$ ($\parallel \hat{z}$)

In this case both longitudinal components as well as planer Hall conductivities are non-zero. The longitudinal components have the following expressions

for Type-I

$$\sigma_{xx}^{(B^2, \Omega)}(\omega) = \sigma_1^{(B^2)} \left[(8 + 13t_s^2) \cos^2 \gamma + \sin^2 \gamma \right] \quad (54)$$

$$\sigma_{zz}^{(B^2, \Omega)}(\omega) = \sigma_1^{(B^2)} (1 + 7t_s^2) \quad (55)$$

for Type-II

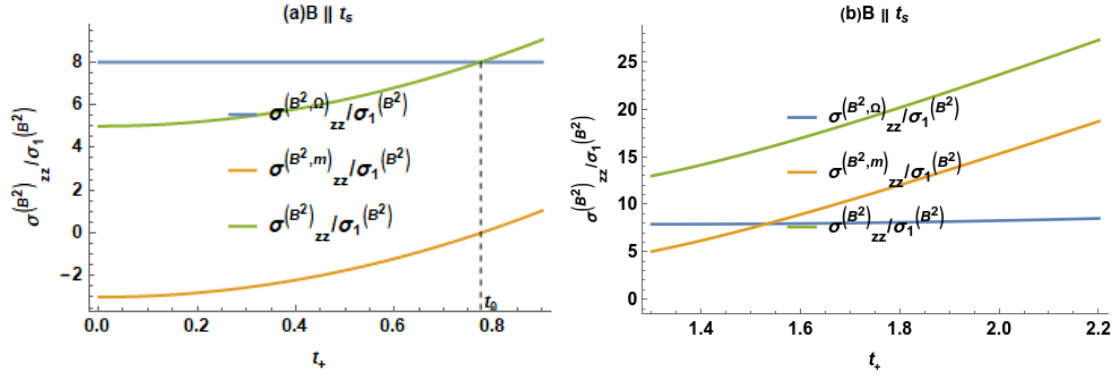


FIG. 10. The dependence of the optical conductivity on the tilt t_+ for the case of $B \parallel t_s$ for (a) type-I WSM and (b) type-II WSM. The other parameters are the same as those of Fig.(1)

$$\begin{aligned} \sigma_{xx}^{(B^2, \Omega)}(\omega) = & \frac{\sigma_1^{(B^2)}}{16t_s^5} \left[\left\{ -55\tilde{\Lambda}_k^{-6} + 48(-4 + t_s^2)\tilde{\Lambda}_k^{-5} - 15(33 - 27t_s^2 + 4t_s^4)\tilde{\Lambda}_k^{-4} - 80(4 - 5t_s^2 + t_s^4)\tilde{\Lambda}_k^{-3} - 165(-1 + t_s^2)^2\tilde{\Lambda}_k^{-2} \right. \right. \\ & + (1 + t_s^2)\{11 - 50t_s^2 + t_s^4(115 + 4|t_s|(8 + 15|t_s|))\} \left. \right\} \cos^2 \gamma + \left\{ -5\tilde{\Lambda}_k^{-6} + 15(-3 + t_s^2)\tilde{\Lambda}_k^{-4} - 15(-1 + t_s^2)^2\tilde{\Lambda}_k^{-2} \right. \\ & \left. \left. + \{1 + 5t_s^2(-1 + 3t_s^2 + t_s^4)\} \right\} \sin^2 \gamma \right] \end{aligned} \quad (56)$$

$$\sigma_{zz}^{(B^2, \Omega)}(\omega) = \frac{\sigma_1^{(B^2)}}{8t_s^5} \left[10\tilde{\Lambda}_k^{-6} + 15(6 - 7t_s^2 + t_s^4)\tilde{\Lambda}_k^{-4} - 30(-1 + t_s^2)^3\tilde{\Lambda}_k^{-2} + \{-2 + 11t_s^2 - 25t_s^4 + 65t_s^6 + 15t_s^8\} \right] \quad (57)$$

The off-diagonal components of conductivities

for Type-I

$$\sigma_{xy}^{(B^2, \Omega)}(\omega) = \sigma_1^{(B^2)}(7 + 13t_s^2) \sin \gamma \cos \gamma \quad (58)$$

for Type-II

$$\begin{aligned} \sigma_{xy}^{(B^2, \Omega)}(\omega) = & \frac{\sigma_1^{(B^2)}}{8t_s^5} \left[-25\tilde{\Lambda}_k^{-6} + 24(-4 + t_s^2)\tilde{\Lambda}_k^{-5} - 15(-5 + t_s^2)(-3 + 2t_s^2)\tilde{\Lambda}_k^{-4} - 40(4 - 5t_s^2 + t_s^4)\tilde{\Lambda}_k^{-3} - 75(-1 + t_s^2)^2\tilde{\Lambda}_k^{-2} \right. \\ & \left. + \{5 - 17t_s^2 + t_s^4\{25 + |t_s|(16 + |t_s|(85 + 2|t_s|(8 + 15|t_s|))\}\} \right] \sin \gamma \cos \gamma \end{aligned} \quad (59)$$

The magnetic orbital moment contributions of conductivities

for Type-I

$$\sigma_{xx}^{(B^2, m)}(\omega) = \sigma_1^{(B^2)} \left[(-3 - 6t_s^2) \cos^2 \gamma - \sin^2 \gamma \right] \quad (60)$$

$$\sigma_{zz}^{(B^2, m)}(\omega) = \sigma_1^{(B^2)}(-1 + t_s^2) \quad (61)$$

$$\sigma_{xy}^{(B^2, m)}(\omega) = \sigma_1^{(B^2)}(-2 - 6t_s^2) \sin \gamma \cos \gamma \quad (62)$$

for Type-II

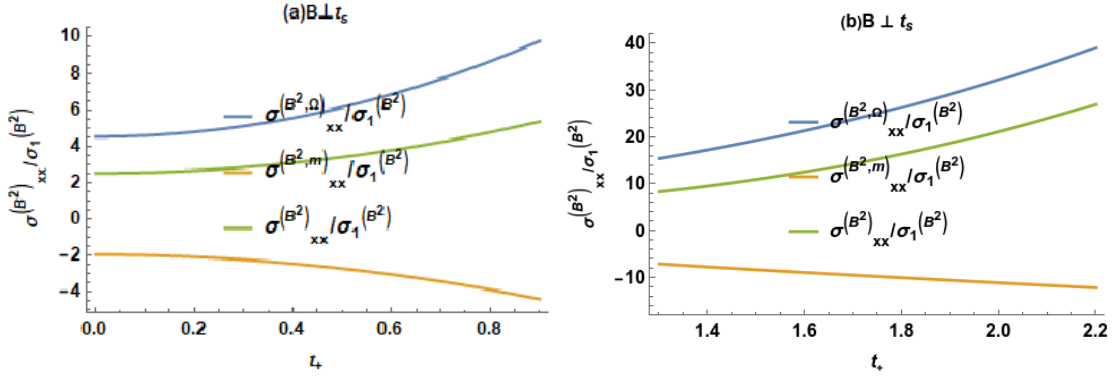


FIG. 11. The dependence of the optical conductivity on the tilt t_+ for the case of $B \perp t_s$ for (a) type-I WSM and (b) type-II WSM at $\theta = \frac{\pi}{4}$. The other parameters are the same as those of Fig.(12)

$$\begin{aligned} \sigma_{xx}^{(B^2, m)}(\omega) = & \frac{\sigma_1^{(B^2)}}{8t_s^5} \left[\left\{ 40\tilde{\Lambda}_k^{-6} - 24\tilde{\Lambda}_k^{-5} + 15(24 + t_s^2)\tilde{\Lambda}_k^{-4} + 40(-1 + t_s^2)\tilde{\Lambda}_k^{-3} - 30(-4 + t_s^2 + 3t_s^4)\tilde{\Lambda}_k^{-2} \right. \right. \\ & - 8 + 7t_s^2 + 30t_s^4 - 16|t_s|^5 - 85t_s^6 \left. \right\} \cos^2 \gamma + 2 \left\{ 10\tilde{\Lambda}_k^{-6} + 12\tilde{\Lambda}_k^{-5} - 15(-6 + t_s^2)\tilde{\Lambda}_k^{-4} + 20\tilde{\Lambda}_k^{-3} - 30(-1 + t_s^2)\tilde{\Lambda}_k^{-2} \right. \\ & \left. \left. - 2 + 5t_s^2 - 12|t_s|^5 + 5t_s^6 \right\} \sin^2 \gamma \right] \end{aligned} \quad (63)$$

$$\sigma_{zz}^{(B^2, m)}(\omega) = \frac{\sigma_1^{(B^2)}}{2t_s^5} \left[-15\tilde{\Lambda}_k^{-6} + 15(-9 + t_s^2)\tilde{\Lambda}_k^{-4} + 45(-1 + t_s^2)\tilde{\Lambda}_k^{-2} + 3 - 8t_s^2 + 5t_s^4 \right] \quad (64)$$

$$\begin{aligned} \sigma_{xy}^{(B^2, m)}(\omega) = & \frac{\sigma_1^{(B^2)}}{8t_s^5} \left[20\tilde{\Lambda}_k^{-6} - 48\tilde{\Lambda}_k^{-5} + 45(4 + t_s^2)\tilde{\Lambda}_k^{-4} + 40(-2 + t_s^2)\tilde{\Lambda}_k^{-3} + 30(2 + t_s^2 - 3t_s^4)\tilde{\Lambda}_k^{-2} \right. \\ & \left. - 4 - 3t_s^2 + 30t_s^4 + 8|t_s|^5 - 95t_s^6 \right] \sin \gamma \cos \gamma \end{aligned} \quad (65)$$

It is noted that all the other magnetoconductivity components are zero. It is clear that the above conductivity equations are independent of chirality, i.e., the Weyl cones with opposite chiralities have the same contribution to the conductivity. The conductivity component $\sigma_{xx}^{(B^2, m)}(\omega)$ for type-I and type-II are always negative, a result that will suppress the total conductivity compare to its Berry curvature parts[see Fig(11)]. Further, the conductivity component $\sigma_{zz}^{(B^2, m)}(\omega)$ for type-I/II is always negative/positive, a result that will suppress/enhance the total conductivity compare to its Berry curvature parts[see Fig(12)].

In the present system, the planar Hall effect can take place and manifest itself in a nonzero conductivity

$\sigma_{xy}^{(B^2)}(\omega)$ [51, 59–65]. Similar to the diagonal components of the conductivity, $\sigma_{xy}^{(B^2)}(\omega)$ also consists of the contributions from the Berry curvature and the orbital magnetic moment. Figure(13) shows an effect of the tilt on the planar Hall magnetoconductivity. It is seen that the total planar Hall conductivity is suppressed in the case of type-I and type-II WSMs when the orbital magnetic moment is present as shown in Fig.(13). Figure (14) shows the planar Hall magnetoconductivity as a function of the THz incident light at $\gamma = \pi/4$. The real and imaginary parts of total conductivities are suppressed due to negative contribution of real and imaginary parts of magnetic orbital moment conductivities.

D. Hall conductivities $\sigma_{ab}^{(H,0)}$ and $\sigma_{ab}^{(H,B)}$

The intrinsic Hall effect is engendered by the Berry curvature, as presented by the second term of Eq. (17),

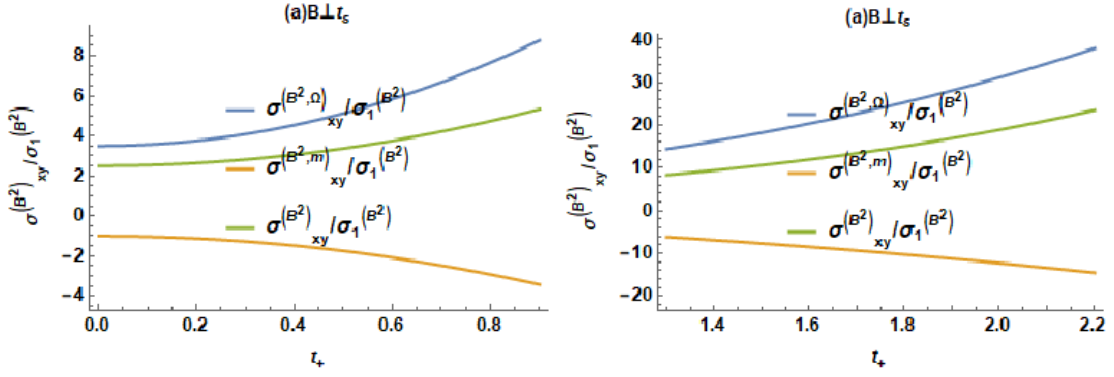


FIG. 13. The dependence of the planar Hall conductivity on the tilt t_+ for the case of $B \perp t_s$, for (a) type-I WSM and (b) type-II WSM at $\theta = \frac{\pi}{4}$. The other parameters are the same as those of Fig.(1)

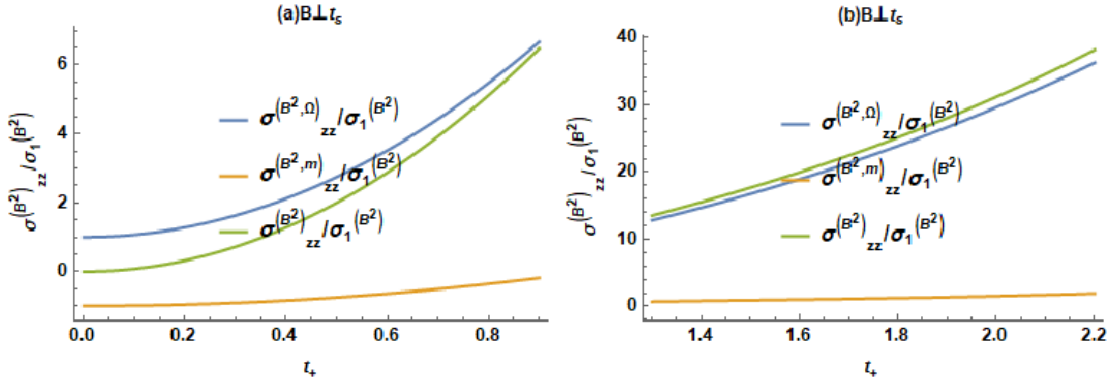


FIG. 12. The dependence of the optical conductivity on the tilt t_+ for the case of $B \perp t_s$ for (a) type-I WSM and (b) type-II WSM. The other parameters are the same as those of Fig.(1)

for which further calculation gives

$$\sigma_{ab}^{(H)} = \sigma_{ab}^{(H,0)} + \sigma_{ab}^{(H,B)} \quad (66)$$

where

$$\sigma_{ab}^{(H,0)}(\omega) = -\frac{e^2}{\hbar(2\pi)^3} \epsilon_{abc} \int d^3k \Omega_c^s f_0^s \quad (67)$$

$$\sigma_{ab}^{(H,B)}(\omega) = \frac{e^2}{\hbar(2\pi)^3} \epsilon_{abc} \int d^3k \Omega_c^s (\mathbf{m}_{\mathbf{k}}^s \cdot \mathbf{B}) \left(\frac{\partial f_0^s}{\partial \epsilon_{\mathbf{k}}^s} \right) \quad (68)$$

where ϵ_{abc} is the Levi-Civita symbol with $a, b, c, \in x, y, z$. The first term $\sigma_{ab}^{(H,0)}(\omega)$ in Eq. (66), referring to the anomalous Hall effect, is not equivalent to zero only in the system with broken time-reversal symmetry [14, 50]. While the second term $\sigma_{ab}^{(H,B)}(\omega)$ stands for the ordinary Hall conductivity linear in B , which is the counterpart to a semiclassical description related to Landau level formation in the quantum limit [49].

Let the magnetic field in spherical polar co-ordinate

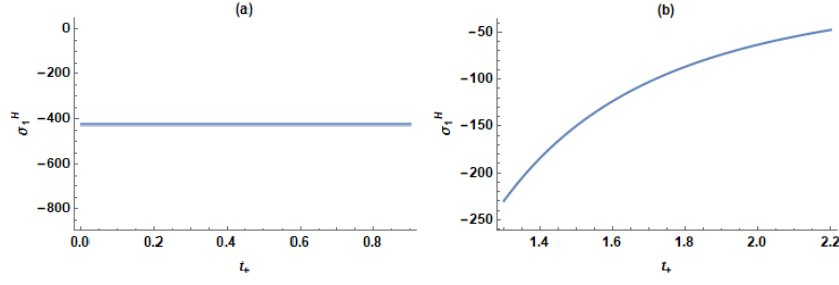


FIG. 15. The dependence of Hall conductivity on the tilt t_+ for (a) type-I WSM and (b) type-II WSM. The other parameters are the same as those of Fig.(1)

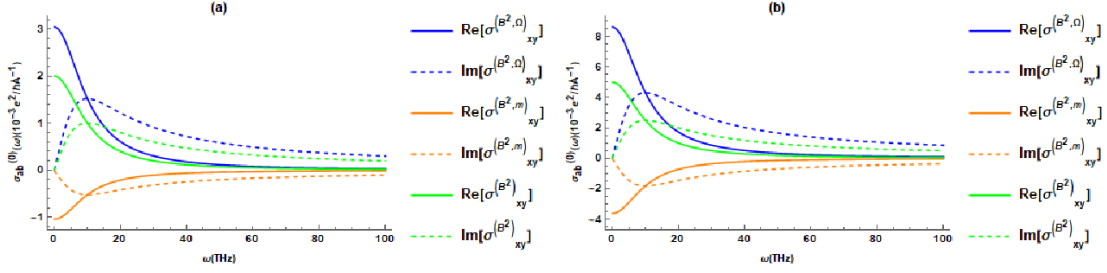


FIG. 14. The frequency dependence of optical conductivity on the tilt for the case of $\mathbf{B} \perp t_s$. for (a) type-I WSM at $t_+ = 0.5$ and (b) type-II WSM at $t_+ = 1.3$, $\theta = \frac{\pi}{4}$ and $B = 1$ T. The other parameters are the same as those of Fig.(1)

system $\mathbf{B} = (B_x, B_y, B_z)$ with $B_x = B \sin \theta \cos \phi$, $B_y = B \sin \theta \sin \phi$, $B_z = B \cos \theta$. For a single Weyl node, the B-linear contribution to the Hall conductivity can be written as

$$\sigma^{(H,B)} = \begin{pmatrix} 0 & \sigma_1^H \cos \theta & -\sigma_1^H \sin \theta \sin \phi \\ -\sigma_1^H \cos \theta & 0 & \sigma_1^H \sin \theta \cos \phi \\ \sigma_1^H \sin \theta \sin \phi & -\sigma_1^H \sin \theta \cos \phi & 0 \end{pmatrix} \quad (69)$$

where

for Type-I

$$\sigma_1^H = -\frac{e^3}{\hbar} \frac{B v_F}{24\pi^2 \mu} \quad (70)$$

for Type-II

$$\sigma_1^H = -\frac{e^3}{\hbar} \frac{B v_F (3\tilde{\Lambda}_k^{-2} + 1)}{24\pi^2 \mu t_s^3} \quad (71)$$

IV. SECOND ORDER NON-LINEAR RESPONSE OF TILTED-WSMS

Now, we explore the second-order nonlinear magneto-optical response of Weyl semimetals. Substituting Eq.(9) into Eq.(10), neglecting the Lorentz force term, and retaining terms up to second order in \mathbf{E} , we obtain

$$\frac{1}{\hbar D} [-e\mathbf{E} - \frac{e^2}{\hbar} (\mathbf{E} \cdot \mathbf{B}) \Omega_k^s] \cdot \frac{\partial \tilde{f}_1^s}{\partial \mathbf{k}} - i\omega \tilde{f}_2^s = -\frac{\tilde{f}_2^s}{\tau} \quad (72)$$

Solve for \tilde{f}_2^s , we obtain

$$\tilde{f}_2^s = \frac{\tau}{(1 - 2i\omega\tau)} \frac{1}{\hbar D} [e\mathbf{E} + \frac{e^2}{\hbar} (\mathbf{E} \cdot \mathbf{B}) \Omega_k^s] \cdot \frac{\partial \tilde{f}_1^s}{\partial \mathbf{k}} \quad (73)$$

In contrast to the type-I WSM node, the B-linear contribution to the Hall conductivity of type-II WSMs depends on the tilt parameter t_s as shown in Fig.(15), the conductivity rises with t_s .

Substituting Eq.(15) into Eq.(73) and retaining terms up to first order in \mathbf{B} , we obtain

$$\begin{aligned} \tilde{f}_2^s &= \frac{e\tau^2}{\hbar(1-i\omega\tau)(1-2i\omega\tau)} \left\{ \mathbf{E} \cdot \frac{\partial}{\partial \mathbf{k}} \left[\left(e\mathbf{E} + \frac{e^2}{\hbar}(\mathbf{E} \cdot \mathbf{B})\Omega_{\mathbf{k}}^s - \frac{e^2}{\hbar}(\mathbf{B} \cdot \Omega_{\mathbf{k}}^s)\mathbf{E} \right) \cdot \mathbf{v}_{\mathbf{k}}^s \frac{\partial f_0^s}{\partial \epsilon_{\mathbf{k}}^s} - \frac{e}{\hbar}\mathbf{E} \cdot \frac{\partial}{\partial \mathbf{k}} \left(\mathbf{m}_{\mathbf{k}}^s \cdot \mathbf{B} \frac{\partial f_0^s}{\partial \epsilon_{\mathbf{k}}^s} \right) \right] \right. \\ &\quad \left. + \left[\frac{e^2}{\hbar}(\mathbf{E} \cdot \mathbf{B})\Omega_{\mathbf{k}}^s - \frac{e^2}{\hbar}(\mathbf{B} \cdot \Omega_{\mathbf{k}}^s)\mathbf{E} \right] \cdot \frac{\partial}{\partial \mathbf{k}} \left(\mathbf{E} \cdot \mathbf{v}_{\mathbf{k}}^s \frac{\partial f_0^s}{\partial \epsilon_{\mathbf{k}}^s} \right) \right\} \end{aligned} \quad (74)$$

Now the electric current density at the frequency 2ω is given by

$$\begin{aligned} j_1 &= -\frac{e}{(2\pi)^3} \int d^3k \left[\tilde{\mathbf{v}}_{\mathbf{k}}^s + \frac{e}{\hbar}(\Omega_{\mathbf{k}}^s \cdot \tilde{\mathbf{v}}_{\mathbf{k}}^s)\mathbf{B} \right] \tilde{f}_2^s \\ &\quad - \frac{e^2}{2\pi)^3\hbar} \int d^3k \mathbf{E} \times \Omega_{\mathbf{k}}^s \tilde{f}_1^s \end{aligned} \quad (75)$$

According to the definition of second harmonic conductivity, this equation should be written in the form

$$\mathbf{j}(2\omega) = \sigma(2\omega)\mathbf{E}(\omega)\mathbf{E}(\omega) \quad (76)$$

where $\sigma(2\omega)$ is the second harmonic conductivity.

A. Second harmonic conductivity σ_{abc}^0 in the absence of magnetic field

In this subsection, we calculate the second harmonic current of the Weyl semimetals system in the absence of

magnetic fields \mathbf{B} . Inserting Eq. (74) into the first term of Eq. (75), the second harmonic conductivity tensor can be written as

$$\sigma_{abc}^0(2\omega) = \frac{-\tau^2}{(1-i\omega\tau)(1-2i\omega\tau)} \frac{e^3}{\hbar(2\pi)^3} \int d^3k \frac{\partial v_a^s}{\partial k_c} v_b^s \left(-\frac{\partial f_0^s}{\partial \epsilon_{\mathbf{k}}^s} \right) \quad (77)$$

Except for the aaz, aza, and zaa ($a = x, y, z$) components of the second harmonic conductivity tensor are nonzero and all other components equal to zero [50, 66]. for Type-I

$$\sigma_{zzz}^0(2\omega) = 2\sigma_{DL} \left[\frac{-6 + 4t_s^2}{t_s^3} - \frac{3(1-t_s^2)}{t_s^4} \ln \frac{1-t_s}{1+t_s} \right] \quad (78)$$

$$\sigma_{xxz}^0(2\omega) = \sigma_{DL} \left[\frac{6}{t_s^3} + \frac{3-t_s^2}{t_s^4} \ln \frac{1-t_s}{1+t_s} \right] \quad (79)$$

for Type-II

$$\sigma_{zzz}^0(2\omega) = \frac{2\sigma_{DL}}{t_s^4} \left[-\tilde{\Lambda}_k^{-2} + (-3 + t_s^2) - 3(-1 + t_s^2) \ln[(t_s^2 - 1)\tilde{\Lambda}_k^2] \right] \quad (80)$$

$$\sigma_{xxz}^0(2\omega) = \frac{\sigma_{DL}}{t_s^4} \left[\tilde{\Lambda}_k^{-2} - (-3 + t_s^2) + (-3 + t_s^2) \ln[(t_s^2 - 1)\tilde{\Lambda}_k^2] \right] \quad (81)$$

where $\sigma_{DL} = \frac{e^3\tau^2\mu}{(1-2i\omega\tau)(1-i\omega\tau)8\pi^2\hbar^3}$ is the Drude-like

frequency dependent complex conductivity.

The second harmonic conductivity tensor satisfies the relation $\sigma_{zxx}^0(2\omega) = \sigma_{zyy}^0(2\omega) = \sigma_{xzx}^0(2\omega) = \sigma_{yzy}^0(2\omega) = \sigma_{xxz}^0(2\omega) = \sigma_{yyz}^0(2\omega)$ and it does not depend on the chirality of Weyl node. The total second harmonic conductivity in tilted Weyl semimetals is the sum of a pair of Weyl nodes. For the case with tilt inversion symmetry $t_+ = -t_-$, $\sigma_{abc}(2\omega) = 0$. For the case with

broken tilt inversion symmetry $t_+ = t_-$, $\sigma_{abc}(2\omega) \neq 0$.

It is noted to see from Fig.(16a) that the $\sigma_{abc}^0(2\omega)$ becomes exactly zero when $t_s \rightarrow 0$ and the presence of the finite tilt is needed to get the second harmonic generation in type-I WSMs. It is also evident from Fig.(16a) that $\sigma_{zzz}^0(2\omega)$ is more sensitive to tilt than $\sigma_{xxz}^0(2\omega)$ in type-I WSMs [50]. Fig.(16b) shows that $\sigma_{zzz}^0(2\omega)$ has opposite behavior with tilt parameter as compare to $\sigma_{xxz}^0(2\omega)$. Fig.(17) shows the frequency variation of tilted-WSMs.

B. Second harmonic conductivity σ_{abc}^B in the presence of linear magnetic field

Inserting Eq. (74) into the first term of Eq. (75), we write the linear \mathbf{B} dependent second harmonic conduc-

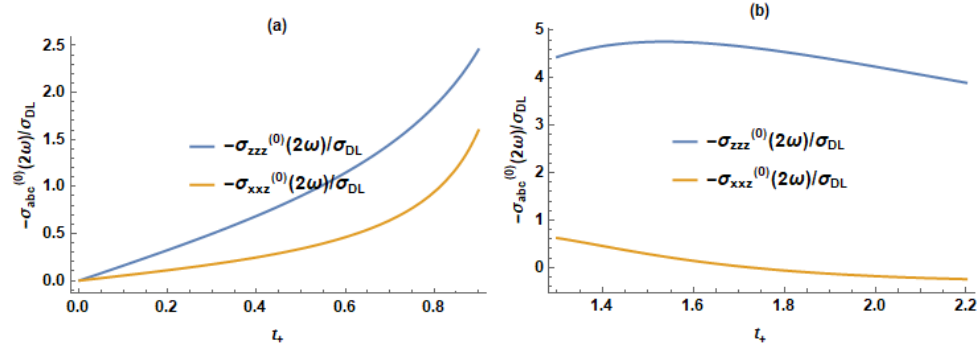


FIG. 16. The dependence of the nonlinear optical conductivities for the process of second harmonic generation of on tilt t_+ for (a) type-I WSM and (b) type-II WSM. Here the relaxation rate $\gamma' = \hbar/\tau$. The other parameters are the same as those of Fig.(1).

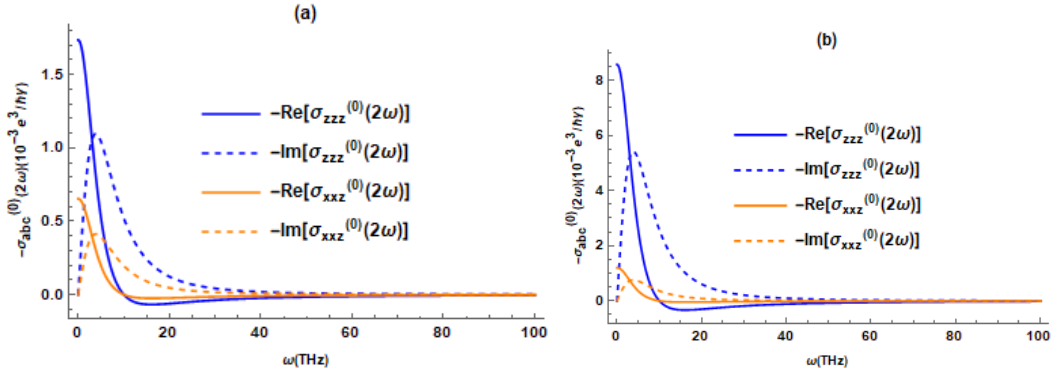


FIG. 17. The frequency dependence of optical conductivity on tilt for the process of second harmonic generation. for (a) type-I WSM at $t_+ = 0.5$ and (b) type-II WSM at $t_+ = 1.3$. The other parameters are the same as those of Fig.(1)

tivity tensor

$$\begin{aligned} \sigma_{abc}^B(2\omega) = & \frac{\tau^2}{(1-i\omega\tau)(1-2i\omega\tau)} \frac{e^3}{\hbar(2\pi)^3} \int d^3k \left\{ \frac{\partial v_a^s}{\partial k_c} \left[-\frac{eB_b}{\hbar} (\Omega_{\mathbf{k}}^s \cdot \mathbf{v}_{\mathbf{k}}^s) + \frac{e v_b^s}{\hbar} (\Omega_{\mathbf{k}}^s \cdot \mathbf{B}) \right] - \frac{eB_c}{\hbar} \frac{\partial}{\partial \mathbf{k}} \cdot (v_a^s \Omega_{\mathbf{k}}^s) v_b^s \right. \\ & \left. + \frac{e}{\hbar} \frac{\partial [v_a^s (\Omega_{\mathbf{k}}^s \cdot \mathbf{B})]}{\partial k_c} v_b^s - \frac{eB_a}{\hbar} \frac{\partial (\Omega_{\mathbf{k}}^s \cdot \mathbf{v}_{\mathbf{k}}^s)}{\partial k_c} v_b^s + \frac{\partial^2 (\mathbf{m}_{\mathbf{k}}^s \cdot \mathbf{B})}{\hbar \partial k_a \partial k_c} v_b^s - \frac{\partial^2 v_a^s}{\hbar \partial k_a \partial k_c} (\mathbf{m}_{\mathbf{k}}^s \cdot \mathbf{B}) \right\} \left(-\frac{\partial f_0^s}{\partial \epsilon_{\mathbf{k}}^s} \right) \end{aligned} \quad (82)$$

We will explore Eq.(82) with following two cases:

for type-I

$$\sigma_{xzx}^B(2\omega) = s \frac{2}{3} \sigma_2^{(B)} \quad (83)$$

$$\sigma_{zxx}^B(2\omega) = -s \frac{2}{3} \sigma_2^{(B)} \quad (84)$$

Case-I In the case of $\mathbf{B} \parallel \hat{t}_s \parallel \hat{z}$, for a single Weyl node, we obtain the magnetoconductivity components

for type-II

$$\begin{aligned} \sigma_{xx}^B(2\omega) = & s \frac{\sigma_2^{(B)}}{15t_s^5} \left[21\tilde{\Lambda}_k^{-5} + 15(7 - 2t_s^2)\tilde{\Lambda}_k^{-4} + 15(14 - 5t_s^2)\tilde{\Lambda}_k^{-3} + 30(7 - 8t_s^2 + t_s^4)\tilde{\Lambda}_k^{-2} \right. \\ & \left. + 15(7 - 7t_s^2 + 2t_s^4)\tilde{\Lambda}_k^{-1} + 21 - 50t_s^2 + 45t_s^4 - 6t_s^6 \right] \end{aligned} \quad (85)$$

$$\begin{aligned} \sigma_{zz}^B(2\omega) = & s \frac{\sigma_2^{(B)}}{240} \left[176 - \frac{210}{|t_s|} - 80 \left(1 - \frac{(\tilde{\Lambda}_k^{-1} - 1)^3}{|t_s|^3} \right) - \frac{210}{|t_s|} \tilde{\Lambda}_k^{-1} \right. \\ & \left. + 55 \cos \left(3 \csc^{-1} \left(\frac{|t_s|}{1 + \tilde{\Lambda}_k^{-1}} \right) \right) - 21 \cos \left(5 \csc^{-1} \left(\frac{|t_s|}{1 + \tilde{\Lambda}_k^{-1}} \right) \right) \right] \end{aligned} \quad (86)$$

where $\sigma_2^{(B)} = \frac{e^4 \tau^2 B v_F^2}{\hbar^2 (1 - 2i\omega\tau)(1 - i\omega\tau) 8\pi^2 \mu}$. We can check that other nonzero second harmonic conductivity components satisfy the relations: $\sigma_{zz}^B(2\omega) = \sigma_{yy}^B(2\omega) = \sigma_{xx}^B(2\omega) = \sigma_{yz}^B(2\omega)$. In contrast to type-I WSMs, the B-linear contribution to the second harmonic conductivity depends on the tilt in type-II WSMs. Summing the conductivity over the Weyl cones with opposite chirality cancels each other, leading to the disappearance of the total B-linear contribution to the second harmonic conductivity.

Case-II In the case of $\mathbf{B} \perp \hat{t}_s$ ($\parallel \hat{z}$), we get the nonzero conductivity components

for type-I

$$\sigma_{xz}^{(B)}(2\omega) = s \frac{2}{3} \sigma_2^{(B)} \cos \gamma \quad (87)$$

$$\sigma_{xz}^{(B)}(2\omega) = -s \frac{2}{3} \sigma_2^{(B)} \cos \gamma \quad (88)$$

$$\sigma_{yz}^{(B)}(2\omega) = s \frac{2}{3} \sigma_2^{(B)} \sin \gamma \quad (89)$$

$$\sigma_{yz}^{(B)}(2\omega) = -s \frac{2}{3} \sigma_2^{(B)} \sin \gamma \quad (90)$$

for type-II

$$\begin{aligned} \sigma_{zz}^{(B)}(2\omega) = & s \frac{\sigma_2^{(B)}}{48|t_s|^3} \left[8 \left\{ 3\tilde{\Lambda}_k^{-4} - 17\tilde{\Lambda}_k^{-3} + 3(5 - 2t_s^2)\tilde{\Lambda}_k^{-2} + 3(-5 + 4t_s^2)\tilde{\Lambda}_k^{-1} + \left\{ 2 + t_s^2(-6 + |t_s|(4 + 3|t_s|)) \right\} \right\} \right. \\ & \left. + \left\{ 11 \cos \left[3 \sec^{-1} \left(\frac{|t_s|}{1 + \tilde{\Lambda}_k^{-1}} \right) \right] - 3 \cos \left[5 \csc^{-1} \left(\frac{|t_s|}{1 + \tilde{\Lambda}_k^{-1}} \right) \right] \right\} \right] \cos \gamma \end{aligned} \quad (91)$$

$$\sigma_{xz}^{(B)}(2\omega) = \frac{\sigma_2^{(B)}}{6|t_s|^3} \left[9\tilde{\Lambda}_k^{-4} + 16\tilde{\Lambda}_k^{-3} + 6(9 - 7t_s^2)\tilde{\Lambda}_k^{-2} - 12(-1 + t_s^2)\tilde{\Lambda}_k^{-1} + 9 - 18t_s^2 - 4|t_s|^3 + 9t_s^4 \right] \cos \gamma \quad (92)$$

$$\begin{aligned} \sigma_{yz}^{(B)}(2\omega) = & \frac{\sigma_2^{(B)}}{48t_s^3} \left[8 \left\{ 3\tilde{\Lambda}_k^{-4} - 17\tilde{\Lambda}_k^{-3} + 3(5 - 2t_s^2)\tilde{\Lambda}_k^{-2} + 3(-5 + 4t_s^2)\tilde{\Lambda}_k^{-1} + \left\{ 2 + t_s^2(-6 + |t_s|(4 + 3|t_s|)) \right\} \right\} \right. \\ & \left. + \left\{ 11 \cos \left[3 \sec^{-1} \left(\frac{|t_s|}{1 + \tilde{\Lambda}_k^{-1}} \right) \right] - 3 \cos \left[5 \csc^{-1} \left(\frac{|t_s|}{1 + \tilde{\Lambda}_k^{-1}} \right) \right] \right\} \right] \sin \gamma \end{aligned} \quad (93)$$

$$\sigma_{yz}^{(B)}(2\omega) = s \frac{\sigma_2^{(B)}}{6|t_s|^3} \left[9\tilde{\Lambda}_k^{-4} + 16\tilde{\Lambda}_k^{-3} + 6(9 - 7t_s^2)\tilde{\Lambda}_k^{-2} - 12(-1 + t_s^2)\tilde{\Lambda}_k^{-1} + 9 - 18t_s^2 - 4|t_s|^3 + 9t_s^4 \right] \sin \gamma \quad (94)$$

In this case, the B-linear contribution to the second harmonic conductivity is dependent on the chirality but independent(dependent) of the tilt in type-I(type-II) WSMs. Summing the conductivity over the Weyl cones with opposite chirality cancels each other, leading to the disappearance of the total B-linear contribution to the second harmonic conductivity.

C. The second order nonlinear Hall conductivity $\sigma_{abc}^{(H,0)}$ in the absence of magnetic field

In this subsection, we study the second-order nonlinear Hall effect of Weyl semimetals without magnetic field. Inserting Eq. (16) into the second term in Eq. (75) and taking $B = 0$, we obtain the nonlinear Hall conductivity.

$$\sigma_{abc}^{(H,0)} = \epsilon_{acd} \frac{e^3 \tau}{\hbar^2 (1 - i\omega\tau)} D_{bd} \quad (95)$$

where D_{bd} is called Berry dipole. It represents the first-order momentum derivative of the Berry curvature, which arises from the uneven distribution of Berry curvature in momentum space[67].

$$D_{bd} = \frac{\hbar}{(2\pi)^3} \int d^3k \Omega_d^s v_b^s \left(-\frac{\partial f_0^s}{\partial \epsilon_{\mathbf{k}}^s} \right) \quad (96)$$

for type-I

$$D_{xx} = D_{yy} = -s \frac{1}{16\pi^2} \left[\frac{2}{t_s} + \frac{1-t_s^2}{t_s^3} \ln \frac{1-t_s}{1+t_s} \right] \quad (97)$$

$$D_{zz} = -s \frac{1}{8\pi^2} \frac{t_s^2-1}{t_s^3} \left[2t_s + \ln \frac{1-t_s}{1+t_s} \right] \quad (98)$$

One can calculate the non-zero components of Berry curvature dipole

for type-II

$$D_{xx} = D_{yy} = s \frac{1}{16\pi^2 |t_s|^3} \left[4\tilde{\Lambda}_k^{-1} - 2t_s + (-1+t_s^2) \ln \left(\frac{|t_s|-1}{|t_s|+1} \right) \right] \quad (99)$$

$$D_{zz} = s \frac{1}{8\pi^2 |t_s|^3} \left[\tilde{\Lambda}_k^{-2} - 3(-1+t_s^2) + \ln \tilde{\Lambda}_k^{-1} - \ln[-1+|t_s|] + (-1+t_s^2) \ln[1+|t_s|] \right. \\ \left. - (-1+t_s^2) \ln \tilde{\Lambda}_k^{-1} + t_s^2 \ln[(-1+|t_s|)\tilde{\Lambda}_k] \right] \quad (100)$$

In contrast to type-I WSMs, the magnitude of Berry curvature dipole components in type-II WSMs depends on chemical potential through momentum cut off. These components depend on the chirality of the Weyl nodes. Therefore, contributions from a pair of Weyl nodes with opposite chirality exactly cancel each other [50, 66, 67].

D. Linear B-contribution to the second order nonlinear Hall conductivity $\sigma_{abc}^{(H,B)}$

Now, we focus on the second-order nonlinear Hall effect in a weak magnetic field. Inserting Eq.(16) into the second term of Eq.(75) and retaining terms up to the first power of B, one obtains complex nonlinear Hall conductivity

$$\sigma_{abc}^{(H,B)} = \epsilon_{acd} \frac{e^3 \tau}{\hbar^2 (1 - i\omega\tau)} [D_{bd}^\Omega + D_{bd}^m] \quad (101)$$

where

$$D_{bd}^\Omega = \frac{e}{(2\pi)^3} \int d^3k \Omega_d^s [B_b (\Omega_{\mathbf{k}}^s \cdot \mathbf{v}_{\mathbf{k}}^s) - v_b^s (\Omega_{\mathbf{k}}^s \cdot \mathbf{B})] \left(-\frac{\partial f_0^s}{\partial \epsilon_{\mathbf{k}}^s} \right) \quad (102)$$

$$D_{bd}^m = \frac{1}{(2\pi)^3} \int d^3k \frac{\partial \Omega_d^s}{\partial k_b} (\mathbf{m}_{\mathbf{k}}^s \cdot \mathbf{B}) \left(-\frac{\partial f_0^s}{\partial \epsilon_{\mathbf{k}}^s} \right) \quad (103)$$

where D_{bd}^Ω and D_{bd}^m are Berry curvature dipole contributions due to the Berry curvature and the orbital

magnetic moment respectively.

Again we will consider the following two cases.

Case I In the case of $\mathbf{B} \parallel \hat{t}_s \parallel \hat{z}$, one obtains the Berry curvature dipole components.

for type-I

$$D_{xx}^\Omega = D_{yy}^\Omega = -t_s D_2^{(B)} \quad (104)$$

$$D_{zz}^\Omega = 2t_s D_2^{(B)} \quad (105)$$

$$D_{xx}^m = D_{yy}^m = 2t_s D_2^{(B)} \quad (106)$$

$$D_{zz}^m = -4t_s D_2^{(B)} \quad (107)$$

for type-II

$$D_{xx}^\Omega = D_{yy}^\Omega = -\frac{D_2^{(B)}}{2t_s^4} \left[3\tilde{\Lambda}_k^{-5} - 5(-3+t_s^2)\tilde{\Lambda}_k^{-3} + 2|t_s|^5 \right] \quad (108)$$

$$D_{zz}^\Omega = \frac{D_2^{(B)}}{t_s^4} \left[3\tilde{\Lambda}_k^{-5} - 5(-3+t_s^2)\tilde{\Lambda}_k^{-3} + 2|t_s|^5 \right] \quad (109)$$

$$D_{xx}^m = D_{yy}^m = \frac{D_2^{(B)}}{8t_s^4} \left[135\tilde{\Lambda}_k^{-4} - 30(-3+t_s^2)\tilde{\Lambda}_k^{-2} - 9 + 10t_s^2 + 15t_s^4 \right] \quad (110)$$

$$D_{zz}^m = -\frac{D_2^{(B)}}{4t_s^4} \left[135\tilde{\Lambda}_k^{-4} - 30(-3+t_s^2)\tilde{\Lambda}_k^{-2} - 9 + 10t_s^2 + 15t_s^4 \right] \quad (111)$$

where $D_2^{(B)} = \frac{1}{8\pi^2} \frac{eB}{\hbar} \frac{\hbar^2 v_F^2}{15\mu^2}$. In contrast to type-I WSMs, the magnitude of Berry curvature dipole components in type-II WSMs depends on chemical potential through momentum cut off.

$$D_{zx}^\Omega = -6t_s D_2^{(B)} \cos \gamma \quad (112)$$

$$D_{xz}^\Omega = 9t_s D_2^{(B)} \cos \gamma \quad (113)$$

$$D_{zy}^\Omega = -6t_s D_2^{(B)} \sin \gamma \quad (114)$$

$$D_{yz}^\Omega = 9t_s D_2^{(B)} \sin \gamma \quad (115)$$

Case-II In the case of $\mathbf{B} \perp \hat{\mathbf{t}}_s$ ($\|\hat{\mathbf{z}}\|$), we get the nonzero components

$$D_{zx}^m = -3t_s D_2^{(B)} \cos \gamma \quad (116)$$

$$D_{zy}^m = -3t_s D_2^{(B)} \sin \gamma \quad (117)$$

for type-I

for type-II

$$D_{zx}^\Omega = -\frac{3D_2^{(B)}}{8t_s^4} \left[5(-3 + t_s^2)\tilde{\Lambda}_k^{-4} - 10(-1 + t_s^2)^2\tilde{\Lambda}_k^{-2} + \left\{ 1 + 5t_s^2(-1 + 3t_s^2 + t_s^4) \right\} \right] \cos \gamma \quad (118)$$

$$D_{xz}^\Omega = \frac{D_2^{(B)}}{4t_s^4} \left[6\tilde{\Lambda}_k^{-5} - 15(-3 + t_s^2)\tilde{\Lambda}_k^{-4} - 10(-3 + t_s^2)\tilde{\Lambda}_k^{-3} - 30(-1 + t_s^2)\tilde{\Lambda}_k^{-2} + \left\{ -3 + 5t_s^2 + t_s^4(15 + |t_s|(4 + 15|t_s|)) \right\} \right] \cos \gamma \quad (119)$$

$$D_{zy}^\Omega = -\frac{3D_2^{(B)}}{8t_s^4} \left[5(-3 + t_s^2)\tilde{\Lambda}_k^{-4} - 10(-1 + t_s^2)^2\tilde{\Lambda}_k^{-2} + \left\{ 1 + 5t_s^2(-1 + 3t_s^2 + t_s^4) \right\} \right] \sin \gamma \quad (120)$$

$$D_{yz}^\Omega = \frac{D_2^{(B)}}{4t_s^4} \left[6\tilde{\Lambda}_k^{-5} - 15(-3 + t_s^2)\tilde{\Lambda}_k^{-4} - 10(-3 + t_s^2)\tilde{\Lambda}_k^{-3} - 30(-1 + t_s^2)\tilde{\Lambda}_k^{-2} + \left\{ -3 + 5t_s^2 + t_s^4(15 + |t_s|(4 + 15|t_s|)) \right\} \right] \sin \gamma \quad (121)$$

and

where

$$D_{zx}^m = \frac{3D_2^{(B)}}{8t_s^4} \left[45\tilde{\Lambda}_k^{-4} - 30(-1 + t_s^2)\tilde{\Lambda}_k^{-2} - 3 + 10t_s^2 - 15t_s^4 \right] \cos \theta \quad |\psi\rangle = \begin{pmatrix} \psi_y \\ \psi_z \end{pmatrix} = \begin{pmatrix} \sin \theta e^{i\alpha_y} \\ \cos \theta e^{i\alpha_z} \end{pmatrix} \quad (125)$$

$$D_{zy}^m = \frac{3D_2^{(B)}}{8t_s^4} \left[45\tilde{\Lambda}_k^{-4} - 30(-1 + t_s^2)\tilde{\Lambda}_k^{-2} - 3 + 10t_s^2 - 15t_s^4 \right] \sin \theta$$

One can check that $D_{zx}^m = D_{xz}^m$ and $D_{zy}^m = D_{yz}^m$ and rest of the components will vanish. In contrast to type-I WSMs, the magnitude of Berry curvature dipole components in type-II WSMs depends on chemical potential through momentum cut off.

is the Jones vector in the y-z plane with phases α_y, α_z and the amplitudes $E_y = |\mathbf{E}| \sin \theta$ and $E_z = |\mathbf{E}| \cos \theta$. Inserting Eq. (124) into Eq. (123), we obtain the nonlinear Hall current

$$j_x(2\omega) = \frac{e^3 \tau}{\hbar^2(1 - i\omega\tau)} \frac{D_{yy}^{(B)} - D_{zz}^{(B)}}{2} \sin 2\theta e^{(\alpha_y + \alpha_z)} |\mathbf{E}|^2 \quad (126)$$

The nonlinear Hall effect can be modulated by the polarization of the incident light, as discussed in Ref.[50]. Using Eq. (101), the electric current is rewritten in the form of

Following the same procedure of Ref.([50]), Eq.(126) can be rewritten as $j_x \sim (D_{yy} - D_{zz})E_y E_z$. Hence conductivity will be

for type-I

$$\mathbf{j}(2\omega) = \frac{e^3 \tau}{\hbar^2(1 - i\omega\tau)} (\hat{\mathbf{D}} \cdot \mathbf{E}) \times \mathbf{E} \quad (123)$$

Assume that an electromagnetic wave propagates in the x direction:

$$\sigma_x^{(H,B)}(2\omega) = \frac{e^3 \tau}{(1 - i\omega\tau)\hbar^2} \frac{3t_s}{2} D_2^{(B)} \sin 2\theta \quad (127)$$

for type-II

$$\mathbf{E}(\mathbf{r}, t) = |\mathbf{E}(\omega)| \text{Re}[\psi] e^{i(qx - \omega t)} \quad (124)$$

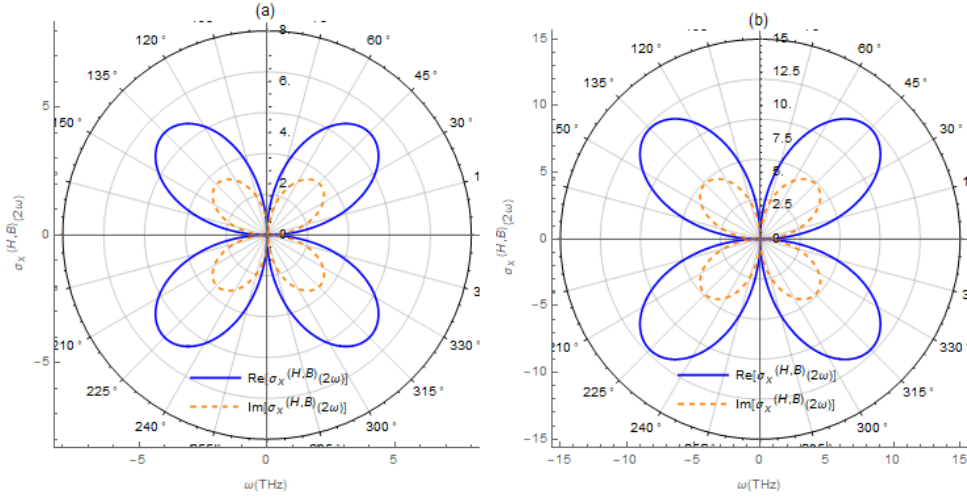


FIG. 19. The angle dependence of the nonlinear Hall conductivity at $\omega = 5$ THz for (a) type-I WSM at $t_+ = 0.5$ (b) type-II WSM at $t_+ = 1.3$. The other parameters are the same as those of Fig.(1)

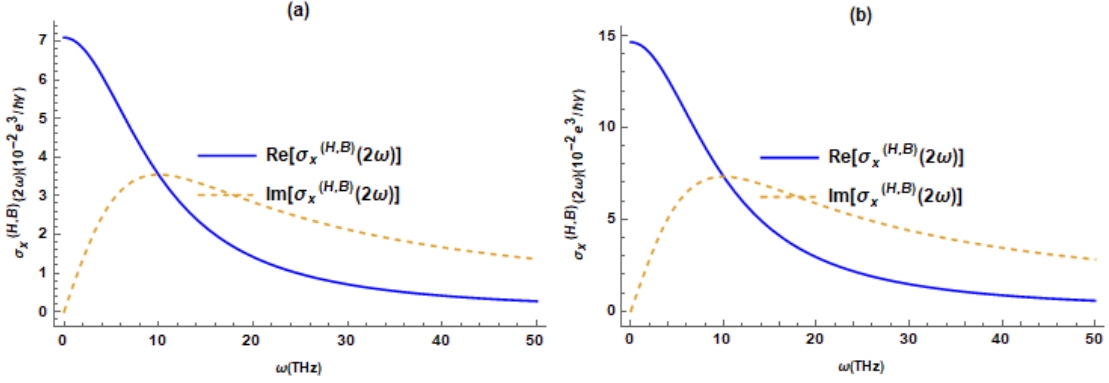


FIG. 18. The nonlinear Hall conductivities for the process of second harmonic generation as a function of the incident photon frequency on the tilt for (a) type-I WSM at $t_+ = 0.5$ (b) type-II WSM at $t_+ = 1.3$. The other parameters are the same as those of Fig.(1)

$$\sigma_x^{(H,B)}(2\omega) = \frac{e^3\tau}{(1-i\omega\tau)\hbar^2} \frac{3}{16t_s^4} \left[-12\tilde{\Lambda}_k^{-5} + 135\tilde{\Lambda}_k^{-4} + 20(-3+t_s^2)\tilde{\Lambda}_k^{-3} - 30(-3+t_s^2)\tilde{\Lambda}_k^{-2} - 9 + 10t_s^2 + 15t_s^4 - 8|t_s|^5 \right] D_2^{(B)} \sin 2\theta \quad (128)$$

Fig.(18) shows the variation of linear-B second harmonic conductivities $\sigma_x^{(H,B)}(2\omega)$ as function of incident photon frequency ω . In contrast to the case of $B = 0$, the

B-linear contribution to the nonlinear Hall conductivity is independent of the chirality and the odd function of t_s . Only in the system with broken tilt inversion symmetry ($t_+ = t_-$), the conductivity $\sigma_x^{(H,B)}(2\omega) \neq 0$.

From Eq.(127) and (128), evidently, $\sigma_x^{(H,B)}(2\omega)$ reaches its maximum when the polarization direction $\gamma = \pm\pi/4$ and vanishes at $\gamma = 0, \pi/2$ as further reflected in Fig(19).

In the nonlinear response regime, a nonlinear Hall effect without external magnetic field is allowed in a bilayer WTe_2 but prohibited in a bulk WTe_2 due to the difference in the crystalline symmetries between them [68, 69]. Recent experiments have measured the non-linear Hall effect in WTe_2 (Type-II Weyl Semimetal) due to its broken inversion symmetry and strong BCD [70]. Type-II WSMs such as $MoTe_2$ display a significant nonlinear Hall effect. The strong tilting of the Weyl points produces a "hot spot" in the Berry curvature, which enhances the BCD. The dipole's contribution to the nonlinear susceptibility can be experimentally detected [71].

V. CONCLUSION

In this work, we have calculated the magneto-optical conductivities of gapless type-II Weyl semimetals in the presence of orbital magnetic moment in linear and non-linear responses within the semiclassical Boltzmann approach and compared their responses existing theoretical work of type-I WSMs. We have found linear B conductivity response along(perpendicular to) tilt direction is suppressed(enhanced) in $\mathbf{B} \parallel \hat{\mathbf{t}}_s$ configuration while planar Hall conductivity is suppressed in $\mathbf{B} \perp \hat{\mathbf{t}}_s$ configuration. Further, we have found quadratic B conductivity responses perpendicular to(along) tilt direction is enhanced(enhanced above t_0) in $\mathbf{B} \parallel \hat{\mathbf{t}}_s$ configuration while planar Hall conductivity is suppressed in $\mathbf{B} \perp \hat{\mathbf{t}}_s$ configuration. However, the non-linear responses are suppressed due to OMM. The magnitudes of conductivity components due to both Berry curvature and OMM have large magnitudes in type-II WSMs due to finite density of states near Weyl points. It is worth mentioning that even though for configuration- a pair of Weyl nodes of opposite chiralities tilted along the arbitrary axis, our results for the linear and non-linear can be generalized to any Weyl configuration with an arbitrary number of pairs of Weyl nodes that are tilted in arbitrary directions, provided that the Weyl nodes are well separated.

Appendix A: DETAILS OF THE CALCULATIONS USING SPHERICAL POLAR COORDINATES

In this paper, we have focused on the n-doped tilted Weyl semimetals with a positive chemical potential μ . In general, one can decompose the momentum \mathbf{k} using

spherical co-ordinates as follow

$$k_x = k \sin \theta \cos \phi \quad (\text{A1})$$

$$k_y = k \sin \theta \sin \phi \quad (\text{A2})$$

$$k_z = k \cos \theta \quad (\text{A3})$$

The general expression for conductivities is given by

$$\begin{aligned} \sigma &= \frac{e^2\tau}{(2\pi)^3} \int_0^\infty k^2 dk \int_0^{2\pi} d\phi_{\mathbf{k}} \int_0^\pi d\theta_{\mathbf{k}} \sin \theta_{\mathbf{k}} f(k, \theta_{\mathbf{k}}, \phi_{\mathbf{k}}) \\ &\times \delta(\mu - \hbar[t_s k \cos \theta_{\mathbf{k}} \pm v_F k]) \end{aligned} \quad (\text{A4})$$

The Jacobian of the transformation is $\mathcal{J} = k^2 \sin \theta_{\mathbf{k}}$, which has been used for analytical expressions of conductivity elements of tilted-WSMs. Substituting $\cos_{\mathbf{k}} \rightarrow x$, the above expression can be rewritten as

$$\begin{aligned} \sigma &= \frac{e^2\tau}{(2\pi)^3} \int_0^\infty k^2 dk \int_0^{2\pi} d\phi_{\mathbf{k}} \int_{-1}^1 dx f(k, x, \phi_{\mathbf{k}}) \\ &\times \delta(\mu - \hbar[t_s k x \pm v_F k]) \end{aligned} \quad (\text{A5})$$

For type-II WSM, we introduce a finite cut-off Λ_k such that $\Lambda_k(1 + t_s) > k_F$ in the radial direction \mathbf{k} . For the conduction band with $t_s > 1$ we obtain the integration limit to be

$$\left(\frac{k_F}{\Lambda_k} - 1\right) \frac{1}{t_s} \leq x \leq 1, \quad (\text{A6})$$

with $\Lambda_k(t_s + 1) > k_F$. The left hand side term of this inequality is negative for $t_s > 0$. When $t_s < -1$, we get

$$-1 \leq x \leq \left(\frac{k_F}{\Lambda_k} - 1\right) \frac{1}{t_s}, \quad (\text{A7})$$

with $\Lambda_k(-t_s + 1) > k_F$. Similarly, we get the following limit for the valence band

$$\left(\frac{k_F}{\Lambda_k} + 1\right) \frac{1}{t_s} \leq x \leq 1, \quad (\text{A8})$$

with $\Lambda_k(t_s - 1) > k_F$ for $t_s > 1$. For $t_s < -1$, we get the following limit

$$-1 \leq x \leq \left(\frac{k_F}{\Lambda_k} + 1\right) \frac{1}{t_s}, \quad (\text{A9})$$

with $-\Lambda_k(t_s + 1) > k_F$. For the calculation of conductivities, all these limits are essential for performing all the integrals.

[1] H. Weyl *et al.*, Electron and gravitation, z. Phys **56**, 330 (1929).

[2] S.-Y. Xu, I. Belopolski, N. Alidoust, M. Neupane, G. Bian, C. Zhang, R. Sankar, G. Chang, Z. Yuan, C.-C.

- Lee, *et al.*, Discovery of a weyl fermion semimetal and topological fermi arcs, *Science* **349**, 613 (2015).
- [3] B. Lv, H. Weng, B. Fu, X. P. Wang, H. Miao, J. Ma, P. Richard, X. Huang, L. Zhao, G. Chen, *et al.*, Experimental discovery of weyl semimetal taas, *Physical Review X* **5**, 031013 (2015).
- [4] L. Lu, Z. Wang, D. Ye, L. Ran, L. Fu, J. D. Joannopoulos, and M. Soljačić, Experimental observation of weyl points, *Science* **349**, 622 (2015).
- [5] H.-J. Kim, K.-S. Kim, J.-F. Wang, M. Sasaki, N. Satoh, A. Ohnishi, M. Kitaura, M. Yang, and L. Li, Dirac versus weyl fermions in topological insulators: Adler-bell-jackiw anomaly? format?; in transport phenomena, *Physical review letters* **111**, 246603 (2013).
- [6] S.-M. Huang, S.-Y. Xu, I. Belopolski, C.-C. Lee, G. Chang, B. Wang, N. Alidoust, G. Bian, M. Neupane, C. Zhang, *et al.*, A weyl fermion semimetal with surface fermi arcs in the transition metal monopnictide taas class, *Nature communications* **6**, 7373 (2015).
- [7] S. Murakami, Phase transition between the quantum spin hall and insulator phases in 3d: emergence of a topological gapless phase, *New Journal of Physics* **9**, 356 (2007).
- [8] X. Wan, A. M. Turner, A. Vishwanath, and S. Y. Savrasov, Topological semimetal and fermi-arc surface states in the electronic structure of pyrochlore iridates, *Physical Review B—Condensed Matter and Materials Physics* **83**, 205101 (2011).
- [9] K.-Y. Yang, Y.-M. Lu, and Y. Ran, Quantum hall effects in a weyl semimetal: Possible application in pyrochlore iridates, *Physical Review B—Condensed Matter and Materials Physics* **84**, 075129 (2011).
- [10] A. Burkov and L. Balents, Weyl semimetal in a topological insulator multilayer, *Physical review letters* **107**, 127205 (2011).
- [11] G. Xu, H. Weng, Z. Wang, X. Dai, and Z. Fang, Chern semimetal and the quantized anomalous hall effect in hgr 2 se 4, *Physical review letters* **107**, 186806 (2011).
- [12] B. Lv, N. Xu, H. Weng, J. Ma, P. Richard, X. Huang, L. Zhao, G. Chen, C. Matt, F. Bisti, *et al.*, Observation of weyl nodes in taas, *Nature Physics* **11**, 724 (2015).
- [13] M. V. Berry, Quantal phase factors accompanying adiabatic changes, *Proceedings of the Royal Society of London. A. Mathematical and Physical Sciences* **392**, 45 (1984).
- [14] D. Xiao, M.-C. Chang, and Q. Niu, Berry phase effects on electronic properties, *Reviews of modern physics* **82**, 1959 (2010).
- [15] H. B. Nielsen and M. Ninomiya, A no-go theorem for regularizing chiral fermions, *Physics Letters B* **105**, 219 (1981).
- [16] S. Borisenko, D. Evtushinsky, Q. Gibson, A. Yaresko, K. Koepernik, T. Kim, M. Ali, J. van den Brink, M. Hoesch, A. Fedorov, *et al.*, Time-reversal symmetry breaking type-ii weyl state in ybmnbi2, *Nature communications* **10**, 3424 (2019).
- [17] X. Huang, L. Zhao, Y. Long, P. Wang, D. Chen, Z. Yang, H. Liang, M. Xue, H. Weng, Z. Fang, *et al.*, Observation of the chiral-anomaly-induced negative magnetoresistance in 3d weyl semimetal taas, *Physical Review X* **5**, 031023 (2015).
- [18] A. C. Potter, I. Kimchi, and A. Vishwanath, Quantum oscillations from surface fermi arcs in weyl and dirac semimetals, *Nature communications* **5**, 5161 (2014).
- [19] P. J. Moll, N. L. Nair, T. Helm, A. C. Potter, I. Kimchi, A. Vishwanath, and J. G. Analytis, Transport evidence for fermi-arc-mediated chirality transfer in the dirac semimetal cd3as2, *Nature* **535**, 266 (2016).
- [20] T. M. McCormick, R. C. McKay, and N. Trivedi, Semiclassical theory of anomalous transport in type-ii topological weyl semimetals, *Physical Review B* **96**, 235116 (2017).
- [21] Y. Ferreiros, A. Zyuzin, and J. H. Bardarson, Anomalous nernst and thermal hall effects in tilted weyl semimetals, *Physical Review B* **96**, 115202 (2017).
- [22] H. B. Nielsen and M. Ninomiya, The adler-bell-jackiw anomaly and weyl fermions in a crystal, *Physics Letters B* **130**, 389 (1983).
- [23] A. Zyuzin and A. Burkov, Topological response in weyl semimetals and the chiral anomaly, *Physical Review B—Condensed Matter and Materials Physics* **86**, 115133 (2012).
- [24] D. T. Son and N. Yamamoto, Berry curvature, triangle anomalies, and the chiral magnetic effect in fermi liquids, *Physical review letters* **109**, 181602 (2012).
- [25] D. Son and B. Spivak, Chiral anomaly and classical negative magnetoresistance of weyl metals, *arXiv preprint arXiv:1206.1627* (2012).
- [26] N. Sinitsyn, Semiclassical theories of the anomalous hall effect, *Journal of Physics: Condensed Matter* **20**, 023201 (2007).
- [27] F. Haldane, Berry curvature on the fermi surface: Anomalous hall effect as a topological fermi-liquid property, *Physical review letters* **93**, 206602 (2004).
- [28] K. Landsteiner, Anomalous transport of weyl fermions in weyl semimetals, *Physical Review B* **89**, 075124 (2014).
- [29] J. H. KIM, Anomalous transport in a weyl metal (The Israel Academy of Science and Humanities, 2022).
- [30] P. Laurell, R. Lundgren, and G. Fiete, Thermoelectric properties of weyl and dirac semimetals, *Bulletin of the American Physical Society* **60** (2015).
- [31] Y. Gao, S. A. Yang, and Q. Niu, Geometrical effects in orbital magnetic susceptibility, *Physical Review B* **91**, 214405 (2015).
- [32] A. Burkov, Negative longitudinal magnetoresistance in dirac and weyl metals, *Physical Review B* **91**, 245157 (2015).
- [33] Q. Chen and G. A. Fiete, Thermoelectric transport in double-weyl semimetals, *Physical Review B* **93**, 155125 (2016).
- [34] Y. Gao, S. A. Yang, and Q. Niu, Intrinsic relative magnetoconductivity of nonmagnetic metals, *Physical Review B* **95**, 165135 (2017).
- [35] A. A. Burkov, Chiral anomaly and transport in weyl metals, *Journal of Physics: Condensed Matter* **27**, 113201 (2015).
- [36] A. A. Zyuzin and R. P. Tiwari, Intrinsic anomalous hall effect in type-ii weyl semimetals, *JETP letters* **103**, 717 (2016).
- [37] J. Steiner, A. Andreev, and D. Pesin, Anomalous hall effect in type-i weyl metals, *Physical review letters* **119**, 036601 (2017).
- [38] A. A. Soluyanov, D. Gresch, Z. Wang, Q. Wu, M. Troyer, X. Dai, and B. A. Bernevig, Type-ii weyl semimetals, *Nature* **527**, 495 (2015).
- [39] P. Li, Y. Wen, X. He, Q. Zhang, C. Xia, Z.-M. Yu, S. A. Yang, Z. Zhu, H. N. Alshareef, and X.-X. Zhang, Evidence for topological type-ii weyl semimetal wte2, *Nature*

- communications **8**, 2150 (2017).
- [40] G. Autes, D. Gresch, M. Troyer, A. A. Soluyanov, and O. V. Yazyev, Robust type-ii weyl semimetal phase in transition metal diphosphides xp_2 ($x = \text{mo, w}$), arXiv preprint arXiv:1603.04624 (2016).
- [41] J. Jiang, Z. Liu, Y. Sun, H. Yang, C. Rajamathi, Y. Qi, L. Yang, C. Chen, H. Peng, C. Hwang, *et al.*, Signature of type-ii weyl semimetal phase in mote_2 , Nature communications **8**, 13973 (2017).
- [42] A. Pal, M. Chinotti, L. Degiorgi, W. J. Ren, and C. Petrovic, Optical properties of ybmnbi_2 : A type ii weyl semimetal candidate, Physica B: Condensed Matter **536**, 64 (2018).
- [43] M. Zhang, Z. Yang, and G. Wang, Coexistence of type-i and type-ii weyl points in the weyl-semimetal osc_2 , The Journal of Physical Chemistry C **122**, 3533 (2018).
- [44] T.-R. Chang, S.-Y. Xu, G. Chang, C.-C. Lee, S.-M. Huang, B. Wang, G. Bian, H. Zheng, D. S. Sanchez, I. Belopolski, *et al.*, Prediction of an arc-tunable weyl fermion metallic state in $\text{mo}_x\text{w}_{1-x}\text{te}_2$, Nature communications **7**, 10639 (2016).
- [45] S.-Y. Xu, N. Alidoust, G. Chang, H. Lu, B. Singh, I. Belopolski, D. S. Sanchez, X. Zhang, G. Bian, H. Zheng, *et al.*, Discovery of lorentz-violating type ii weyl fermions in laalge , Science advances **3**, e1603266 (2017).
- [46] S. Saha and S. Tewari, Anomalous nernst effect in type-ii weyl semimetals, The European Physical Journal B **91**, 4 (2018).
- [47] G. Sharma, P. Goswami, and S. Tewari, Chiral anomaly and longitudinal magnetotransport in type-ii weyl semimetals, Physical Review B **96**, 045112 (2017).
- [48] S. Mukherjee and J. Carbotte, Anomalous dc hall response in noncentrosymmetric tilted weyl semimetals, Journal of Physics: Condensed Matter **30**, 115702 (2018).
- [49] T. Morimoto, S. Zhong, J. Orenstein, and J. E. Moore, Semiclassical theory of nonlinear magneto-optical responses with applications to topological dirac/weyl semimetals, Physical Review B **94**, 245121 (2016).
- [50] Y. Gao, Z.-Q. Zhang, H. Jiang, and K.-H. Ding, Suppression of magneto-optical transport in tilted weyl semimetals by orbital magnetic moment, Physical Review B **105**, 165307 (2022).
- [51] K. Das and A. Agarwal, Linear magnetochiral transport in tilted type-i and type-ii weyl semimetals, Physical Review B **99**, 085405 (2019).
- [52] R. Ghosh and I. Mandal, Direction-dependent conductivity in planar hall set-ups with tilted weyl/multi-weyl semimetals, Journal of Physics: Condensed Matter **36**, 275501 (2024).
- [53] G. Sundaram and Q. Niu, Wave-packet dynamics in slowly perturbed crystals: Gradient corrections and berry-phase effects, Physical Review B **59**, 14915 (1999).
- [54] S. Nandy, C. Zeng, and S. Tewari, Chiral anomaly induced nonlinear hall effect in semimetals with multiple weyl points, Physical Review B **104**, 205124 (2021).
- [55] D. Xiao, J. Shi, and Q. Niu, Berry phase correction to electron density of states in solids, Physical review letters **95**, 137204 (2005).
- [56] E. Malic, T. Winzer, E. Bobkin, and A. Knorr, Microscopic theory of absorption and ultrafast many-particle kinetics in graphene, Physical Review B **84**, 205406 (2011).
- [57] F. M. Pellegrino, M. I. Katsnelson, and M. Polini, Helicons in weyl semimetals, Physical Review B **92**, 201407 (2015).
- [58] H. B. Nielsen and M. Ninomiya, Absence of neutrinos on a lattice:(i). proof by homotopy theory, Nuclear Physics B **185**, 20 (1981).
- [59] A. Burkov, Giant planar hall effect in topological metals, Physical Review B **96**, 041110 (2017).
- [60] S. Nandy, G. Sharma, A. Taraphder, and S. Tewari, Chiral anomaly as the origin of the planar hall effect in weyl semimetals, Physical review letters **119**, 176804 (2017).
- [61] D. Ma, H. Jiang, H. Liu, and X. Xie, Planar hall effect in tilted weyl semimetals, Physical Review B **99**, 115121 (2019).
- [62] N. Kumar, S. N. Guin, C. Felser, and C. Shekhar, Planar hall effect in the weyl semimetal gdptbi , Physical Review B **98**, 041103 (2018).
- [63] J. Yang, W. Zhen, D. Liang, Y. Wang, X. Yan, S. Weng, J. Wang, W. Tong, L. Pi, W. Zhu, *et al.*, Current jetting distorted planar hall effect in a weyl semimetal with ultrahigh mobility, Physical Review Materials **3**, 014201 (2019).
- [64] F. Chen, X. Luo, J. Yan, Y. Sun, H. Lv, W. Lu, C. Xi, P. Tong, Z. Sheng, X. Zhu, *et al.*, Planar hall effect in the type-ii weyl semimetal t d-mot e_2 , Physical Review B **98**, 041114 (2018).
- [65] P. Li, C. Zhang, Y. Wen, L. Cheng, G. Nichols, D. G. Cory, G.-X. Miao, and X.-X. Zhang, Anisotropic planar hall effect in the type-ii topological weyl semimetal wte_2 , Physical Review B **100**, 205128 (2019).
- [66] Y. Gao and B. Ge, Second harmonic generation in dirac/weyl semimetals with broken tilt inversion symmetry, Optics Express **29**, 6903 (2021).
- [67] I. Sodemann and L. Fu, Quantum nonlinear hall effect induced by berry curvature dipole in time-reversal invariant materials, Physical review letters **115**, 216806 (2015).
- [68] Q. Ma, S.-Y. Xu, H. Shen, D. MacNeill, V. Fatemi, T.-R. Chang, A. M. Mier Valdivia, S. Wu, Z. Du, C.-H. Hsu, *et al.*, Observation of the nonlinear hall effect under time-reversal-symmetric conditions, Nature **565**, 337 (2019).
- [69] Z. Du, H.-Z. Lu, and X. Xie, Nonlinear hall effects, Nature Reviews Physics **3**, 744 (2021).
- [70] O. O. Shvetsov, V. D. Esin, A. V. Timonina, N. N. Kolesnikov, and E. Deviatov, Nonlinear hall effect in three-dimensional weyl and dirac semimetals, JETP letters **109**, 715 (2019).
- [71] Y. Zhang, Y. Sun, and B. Yan, Berry curvature dipole in weyl semimetal materials: An ab initio study, Physical Review B **97**, 041101 (2018).